UNIVERSITY OF CALIFORNIA,
IRVINE

Life Cycle Assessment Comparing Concrete Additive Manufacturing to Conventional Manufacturing of Ultra-Tall Wind Turbine Towers

THESIS

submitted in partial satisfaction of the requirements
for the degree of

MASTER OF SCIENCE

in Civil and Environmental Engineering

by

Kathryn Eileen Sheehan Jones

Thesis Committee:
Associate Professor Mo Li, Chair
Adjunct Professor Farzad Naeim
Assistant Professor Mohammad Javad Abdolhosseini Qomi

2022

DEDICATION

To my parents and the many postcards they sent me

TABLE OF CONTENTS

Page

LIST OF FIGURES

LIST OF TABLES

ACKNOWLEDGEMENTS

I would like express my deepest thanks to my committee chair, Professor Mo Li, for her keen insight into the developing world of concrete additive manufacturing and her continuous support of my work and professional development within the constraints some very unconventional virtual few years. Her support and guidance was crucial to the success of this thesis, and is a constant inspiration on work to come.

I would also like to thank my committee members, Professor Farzad Naeim and Professor MJ Qomi, whose shared professional experiences are both educational and inspiring, serving as bright examples of the impressive range of civil engineering specialties and elucidating on how everything in the field works together, from the smallest atom to the tallest skyscraper.

I would like to thank Gary Barter and Pietro Bortolotti at NREL as well as Dennis Janda at Broadwind for the technical advice and assistance they provided that helped make this report as accurate as possible.

In addition, I'd like to thank Jason Cotrell for his part in encouraging me to pursue a program in concrete additive manufacturing, and for inspiring me with his passionate drive for creating viable 3D printed wind turbine towers for a greener future. I'd also like to thank Gabriel Falzone at RCAM for all of his assistance over the development of this research, as well as Zhi-Yuan Cheng at WSP for sharing the structural design process and results on concrete printed towers with me for this research. I would also like to acknowledge the funding support by California Energy Commission under Prime Agreement No. EPC-19-007 for this research.

ABSTRACT OF THE THESIS

Life Cycle Assessment Comparing Concrete Additive Manufacturing to Conventional Manufacturing of Ultra-Tall Wind Turbine Towers

by

Kathryn Eileen Sheehan Jones

Master of Science in Civil and Environmental Engineering

University of California, Irvine, 2022

Associate Professor Mo Li, Chair

Wind power is a quickly growing renewable energy resource within the continental United States and is expected to continue increasing as more wind farms are installed on and off shore. Large wind turbines benefit from economy of scale from larger components such as taller towers. However, onshore turbine development is hindered by conventional transportation restrictions which limit the diameter and weight of the tower segments. The average height of conventional wind turbine towers installed in the U.S. is slightly over 80 m tall. An ultra-tall 140 m tower would increase the amount of energy produced by more than 21% at a site with moderate wind shear, but is a challenge to construct based on conventional transportation size limits.

One proposed solution to this problem is to employ concrete additive manufacturing technology to build ultra-tall wind turbine towers on site. To gauge the potential environmental impacts of this approach, this study performed a life cycle assessment (LCA) comparing the environmental impacts of for four prototype 7.5 MW wind turbine towers with hub heights of 140 m: a conventional tubular steel tower assembled using bolted connections, a concrete tower with segments prefabricated with high-strength (78 MPa) 3D printed shells and precast off-site

with normal-strength (35 MPa) concrete with final assembly on-site, a concrete tower additively manufactured on-site using normal-strength (35 MPa) concrete, and a concrete tower additively manufacture on-site using high-strength (78 MPa) concrete. The steel tower was designed similar to National Renewable Energy Laboratory's (NREL) adapted 5 MW Big Adaptive Rotor (BAR) project, with a power rating scaled from 150 W/m^2 up to 229 W/m^2 to better match California's moderate wind speeds. The concrete towers were designed using the ASCE-7-16 direct winds and dynamic turbine wind loads, in combination with other important loading such as dead load and seismic load. For all four towers, five stages of life cycle assessment were considered: material production, transportation, construction, use, and end of life. A life cycle inventory was developed to catalog the inputs (e.g. raw materials and energy) and outputs (e.g. emissions to air) associated with each tower's life cycle. The input variables for the LCA incorporated the differences in the tower materials, structural designs, and manufacturing methods.

The results of this study indicate that compared with the steel tower, the concrete tower additively manufactured on-site with 35 MPa concrete will have 24% lower CO_2 emissions and 26% higher energy consumption; however, the concrete tower additively manufactured on-site with 78 MPa concrete will have 15% higher CO_2 emissions and 62% higher energy consumption than the steel tower. The difference is due to the significantly higher cement content in the 78 MPa concrete than the 35 MPa concrete. Cement is the most energy-intensive ingredient in concrete and is responsible for most of the greenhouse gas emissions of concrete. The results also show that compared with a concrete tower with sections prefabricated off-site and assembled on-site, a concrete tower that is additively manufactured on-site has a 25% reduction in CO_2 emissions attributed to both the transportation and materials phases. Furthermore, among the five stages of the life cycle, the material production stage dominated and was found to contribute over 92% of

the total CO_2 emissions and 67-93% energy consumptions of each tower. This is due to the large volume of materials used for the ultra-tall towers, and relatively low need for repairs and maintenance during the tower's life cycle. A parametric study was conducted for the on-site additively manufactured towers and revealed the strong effect of cement percentage in the concrete on the CO_2 emissions of the tower. Additional parametric studies were conducted for the other four life cycle stages to examine the effects of variables including the distance from the concrete plant to tower construction site, the size and number of tower segments, rated tower life, and tower end-of-life recycling rate.

The results highlight the need for future development of environmentally friendly 3D printing concrete materials for ultra-tall tower applications. Low-energy and low-CO_2 concrete that incorporates waste or recycled products and can be additively manufactured will significantly reduce the environmental impacts of ultra-tall turbine towers. If the 3D printing concrete can possess high strength, it will also lead to more efficient structural designs that use less concrete, further reducing the environmental impacts. The results reveal an opportunity for further research and development of concrete additive manufacturing technology for the wind energy applications including towers, foundations and energy storage.

1. Introduction

Renewable energy is a quickly growing field with a marked impact on societal well-being. Dramatic weather events that occur with increased frequency have made environmental policy a focus of social and political debate and reform in recent years, with higher degrees of environmental awareness and involvement being displayed by the worldwide society at large [1,2]. As fossil fuels have made up the largest single contributor to current global climate change, renewable energy can be interpreted as one of the most important necessities in reducing the global carbon footprint [3,4].

One of the largest subsets of modern renewable energy technology is wind power. In 2018 wind energy accounted for 6.5% of total U.S. electricity production, and had an 8% increase in power capacity from the prior year, and by 2020 wind supplied 8.3% of electricity within the U.S. with capacity being added at a record pace [5,6]. This number is expected to increase as more wind farms are installed on and off shore, and as more advanced wind turbines capable of generating more power are designed and launched [7]. Energy analysists have projected that within the U.S. the wind energy capacity will experience annual additions of 11 to 13 GW in both 2024 and 2025 [6]. One documented way turbines can harness more power is by increasing the height of the tower to access stronger and more consistent winds [8]. The average conventional wind turbine tower currently installed in the U.S. is just over 80 meters tall, and is a steady increase from the initial tower heights of less than 40 meters in the 1990s [8,9]. As technology and infrastructure develops, turbines use longer blades (i.e., from less than 40 m rotor diameters in the early 2000's to over 100 m diameters in 2020) to generate more power, which in turn requires taller towers that can support the blades and lift them into stronger air streams [6]. Should a tower grow to 140 meters or over,

it would be able to access higher and stronger winds which could increase the amount of energy produced by over 20% at a site with moderate wind shear [10], making taller turbines an attractive opportunity with potential for development in all 50 states in the U.S., as seen in Figure 1 [11]. Off-shore turbines already can reach heights of up to 100 meters, and are projected to reach 150 meters (500 feet) by 2035 [8].

However, a challenge facing ultra-tall onshore towers is transportation; taller turbine towers require wider diameters, which are difficult to transfer through conventional highway overpasses and train tunnel height limits [12]. For blades, the National Renewable Energy Lab (NREL) has been developing designs and materials, such as segmented designs or materials made using glass and carbon fiber composites, that would allow the blades to bend and flex so that they can be transported by rail [13]. As for the towers themselves, the maximum diameter of a land-based wind turbine component in the United States that requires land transportation is approximately 4.3 meters, which is dictated by highway and rail overpass heights [12]. Wind turbine towers beyond those limits must be either transported in smaller pieces that meet the 4.3 m transportation limit, or are confined to off-shore development. This constraint has inspired a variety of engineering approaches to continue the development of large-scale land-based wind turbines [14,15,18-20].

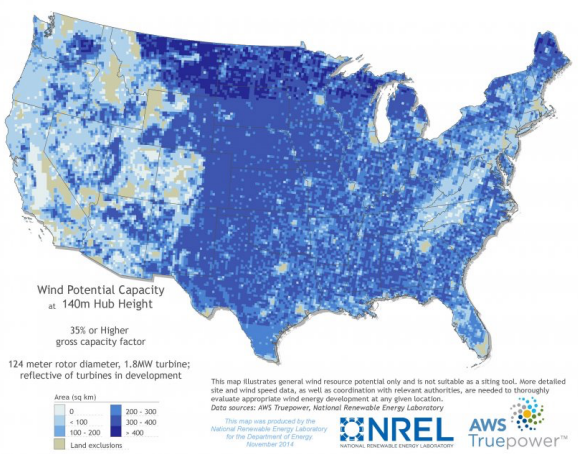

Figure 1 - Wind Potential Capacity within the continental United States at hub heights of 140 m. [11]

Traditionally, wind turbine towers are designed using rolled steel tubes, also referred to in the industry as sections, which are individually transported to the tower site via rail or specialized heavy haul trailers and then stacked on top of one another using cranes at the build site. These sections are then welded or bolted together for stability before the nacelle and blades are deposited safely on top. However, with the increasing height scale, this traditional approach to turbine design faces some notable drawbacks, namely a constrained diameter that requires a larger steel thickness with higher strength steel, or a modified design comprised of segmented base sections that must be assembled on the tower build site [14-16]. To avoid those constraints some large-scale turbines utilize a hybrid design, combining both concrete and steel tower components to assemble the finished tower. This method of tower design is common for towers with heights above 120 meters [12]. In a hybrid tower, the lower portion, typically the first ~90 m of the tower, is constructed out of reinforced concrete, forming in essence an elevated base upon which the final steel portion, which can be 50-80 m, is stacked. This eliminates the need for steel sections with diameters larger than 6 meters or diameter to thicknesses ratios smaller than 100 that can make rolling the steel into

sections an expensive and difficult task. In order for the concrete sections of a hybrid tower to avoid this transportation limit, they are commonly cast in the factory as 3 to 4 arc segments with a 4 m height that can be transported via flatbeds and bolted together on-site, before being moved into place as a single circular section by the cranes [15]. While both the fully steel and traditional hybrid towers have been utilized in industry, both are still subject to transportation limits as well as increasing costs as the weight and thickness of the towers increases [17]. From this limitation several innovative approaches to develop ultra-tall wind turbine towers have arisen.

One novel approach is the Hexcrete tower concept developed by Iowa State University [18]. The Hexcrete approach is to construct a concrete tower out of rectangular, tapered reinforced concrete panels connected via posttensioned hexagonal columns. The panels and columns are designed to be easy to prefabricate in comparison to the traditional concrete sections made for hybrid towers, which require extensive formwork as well as careful match casting to ensure each section perfectly aligns with its conjoining neighbors. In addition, the tower assembly and erection process can be varied, by either assembling more traditionally with stacked Hexcrete cells (Figure 2), or by stacking the columns to a certain height and post tensioning before attaching the connecting panels. Hexcrete can take advantage of advanced concrete materials such as high-performance concrete (HPC), high-strength concrete (HSC), or ultra-high-performance concrete (UHPC). So far, an initial concept Hexcrete cell has been built to scale and subjected to loads representing the operational, extreme, and ultimate limit states of the top 3.6 m portion of a 120-meter-tall tower [18,19]. Since these structural experiments took place in 2015, additional Hexcrete research is being performed towards the design of a 140 m tall Hexcrete tower for 2.3 MW and 3.2 MW Siemens turbines [20], as well as development of a commercialization plan to promote the technology within the wind-energy industry.

Another unconventional approach to tall onshore wind towers made of steel is spiral welding. Spiral welding is a construction technology commonly utilized in the pipe and piling industry, and is performed by converting a long steel sheet or sheets into a cylindrical tube via curling the metal at an angle and welding the edges together. One of the major advantages of using this method for constructing turbine towers is being able to design a steel tower with an unconstrained maximum diameter, which has great weight-saving potential, while a major challenge is ensuring the top and bottom cuts of the tower are perfectly in parallel with one another. Keystone tower systems has developed a machine capable of taking a constant-thickness steel plate and producing a tapered, rolled tubular wind turbine tower (Figure 2) [21]. Since the process takes place using a single machine, spiral welding has the capability of being able to build a complete steel turbine tower at the erection site, eliminating the transport constraints of traditional steel tower assembly. Keystone's first onshore factory was opened in mid 2021 in Pampa, Texas, and has proposed that it will be able to produce a 1 GW per year capacity by mid 2022 by producing 1 MW scale tower per day [22].

Figure 2 - Clockwise from bottom left: Full-scale Hexcrete cell, assembly of Hexcrete tower using preassembled cells, proposed Hexcrete hybrid and fully concrete tower assemblies, Keystone spiral welding tower manufacturing process. [18,21]

Another proposed method for installing the wind turbines on-site is concrete additive manufacturing, also known as concrete 3D printing (3DCP). This technique uses an automatically controlled robotic arm or a gantry printer to deposit concrete layer by layer to manufacture a tower section, followed by erecting and assembling these tower sections through post-tensioning. This method allows on-site, automated construction, eliminates the need for formworks that are conventionally required by concrete casting, and can potentially minimize labor, materials and wastes, and costs. Most importantly, this method addresses the tower diameter size due to the limits of transportation by enabling on-site construction with local concrete ingredients. This approach

can be used to design large scale towers capable of reaching heights and power generation capacities exceeding 140 meters and 7.5 MW, respectively.

The novelty of a concrete additive manufacturing approach means that there is no existing data on the environmental impacts of this type of manufacturing, which is a key consideration when designing new structures specifically made to reduce such impacts. Identifying how a 3DCP wind turbine tower differs from a conventional steel tower of the same height and power rating will illuminate which materials or construction parameters may need additional workshopping to become environmentally viable, or may need to be replaced altogether. This study aims to provide the information necessary to making those decisions prior to the physical construction phase of any future project by utilizing a life cycle assessment framework.

To date wind turbines and their modified designs have been the subject of several life cycle assessment studies and reports. Most are built to compare and contrast different tower or blade designs and processes. Comparisons are applications where life cycle assessment can be well utilized, as they can highlight specific parameters within differing tower designs that have notable emission differences, and are therefore areas worth focusing on for future development and research. Life cycle assessment can also be used to justify an existing technology, and have been used previously to quantify wind energy's environmental impacts from cradle to grave [23]. Other studies have compared wind energy to conventional power generation methods such as coal, oil, hydro, and nuclear. In one such study a 4.5 MW wind turbine with a 124 m concrete tower was the subject of a LCA aiming to quantify the environmental viability of wind turbines [24]. The study validated their findings by comparing the energy intensity of a wind turbine to the energy intensity of fossil fuels and nuclear energy, and investigating the LCA emissions of the turbine.

Beyond the arc welding approach to making larger scale steel towers, there are LCA studies that have investigated lattice designs of steel wind turbine towers, citing the potential of 35% less steel and a 33% lighter foundation at heights of 76 m, with ongoing research into the performance of taller lattice towers [25]. Traditional tubular steel towers are susceptible to buckling at thinner wall thicknesses, and therefore thicker, heavier sections are often unavoidable. Based on the study results, lattice designs may use less total energy to transport and manufacture than tubular turbines.

Wind turbine hub height is a specific area of focus in several published life cycle assessments. In one particularly relevant two-part report three tubular onshore wind turbine towers made of steel, concrete, and a hybrid steel-concrete design were analyzed at three different hub heights varying from 80 to 150 meters tall [16, 26]. Three end of life scenarios were also considered, including recycling the towers, refurbishing and refitting the towers, and relocating the towers after their initial 20-year lifespan was concluded. The report focused on the differences in performance between the towers, as well as comparing the traditional bolted fittings between steel sections to a friction connection. For the initial 20-year lifespan scenario of the 150 m towers, the concrete tower had the majority of lowest environmental impact categories, with one of the steel tower designs narrowly having a lower global warming potential. This study validates the possibility that concrete wind tower turbines at heights above 100 meters have the potential to be environmentally competitive against steel and hybrid designs.

This report aims to address the question of how three different concrete 3D printed wind turbine towers, with sections made of solid printed material or sections made using printed shells filled with cast concrete, would compare to a fully steel tower at the novel height of 140 meters, with respect to the environmental emissions generated by each tower over their cradle to grave life cycle. In addition, this research seeks to determine which areas of the tower life cycles can or

should be adjusted to reduce future emissions based on each process or material's contribution to the net emissions of the system. One hypothesis that was tested was that the printed towers would have lower net emissions compared to the steel tower based on the shorter transport distances and processing stages, as well as the comparatively lower global warming emissions of concrete to processed steel by unit weight.

To investigate these research questions a life cycle assessment model was implemented. The life cycle model takes into account each systemic difference between the steel and concrete towers, while allowing shared features (rotor, blade, hub, foundation, internal addons such as stairs) to remain equivalent and thus unconsidered for both systems in this study. Using life cycle assessment framework, each tower design will return a quantative value indicating its emissions; the values collected and reported in this study are global warming potential (GWP), eutrophication, smog, fossil fuel depletion, acidification, and ozone depletion, with their relevant units listed in Table 1. These indicators were selected due to their relevance to global climate change, the reduction of which is the primary goal of the towers discussed in this report.

Table 1 - Environmental indicators for LCA, derived from TRACI impact categories.

Impact Indictor	**Unit**
Ozone Layer Depletion Potential (ODP)	kg CFC-11 Equiv.
Global Warming Potential (GWP)	kg CO_2 Equiv.
Acidification Potential (AP)	kg SO_2 Equiv.
Eutrophication Potential (EP)	kg N Equiv.
Photochemical Smog Creation Potential (POCP)	kg O_3 Equiv.
Fossil Fuel Depletion (FFD)	MJ Surplus

The systems that were modeled for each tower included materials, transport, construction, use, and end of life. The parameters considered were total material volumes and weight, site location, prefabrication locations, crane type, number of tower sections, printing speed, number of workers,

maintenance schedules, end of life material recovery percentages, and the general design choices needed to calculate those parameters. This study will demonstrate the impact each of these systems and parameters has on climate change emissions for concrete 3D printed and steel towers, which in turn will illuminate areas where future research may be valuable to improve the calculated emissions factors.

2. Model Design

2.1 Life Cycle Assessment Methods

Life cycle assessments are methods by which a product or system is quantified based on the various environmental, social, and economic impacts incurred over its life cycle. A complete cycle, often referred to as a "cradle to grave" life cycle, includes steps for material acquisition, processing, manufacturing, use, disposal and end-of-life, be that recycling or waste allocation. These analyses are most useful when used as comparative tools, placing one or more similar systems against one another to highlight how key changes will impact the total product outlook. A complete summary of the various steps taken into consideration in the life cycle assessment considered in this report are listed in Figure 3, with marked indications on areas where LCA comparisons between steel and 3DCP turbine towers are hypothesized to have the greatest variation. The framework of the life cycle assessment in this report follows the international standards ISO 14040 (2006) [27] and ISO 14044 (2006) [28].

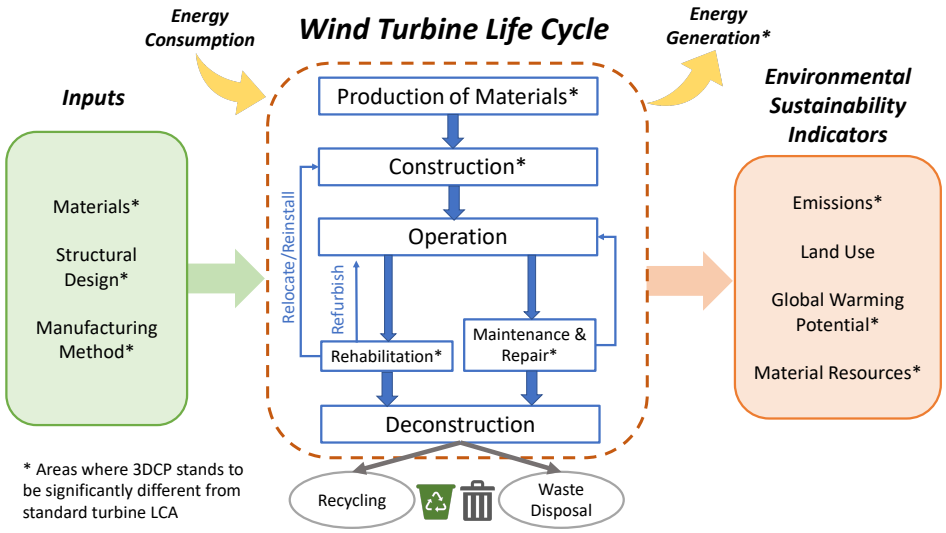

Figure 3 – Cradle to grave life cycle of a wind turbine tower.

2.2 Design Assumptions

This study considered three types of ultra-tall wind turbine towers with the same height of 140 m and a power rating of 7.5 MW. The input variables are the tower materials, structural designs, and manufacturing methods. The first type of wind turbine tower considered in this report is a steel tower, primarily composed of cylindrical rolled steel sections that are assembled into the complete tower via stacking each section upon the next and securing it in place by bolting the flanges together. The steel tower was designed similar to NREL's adapted 5-MW Big Adaptive Rotor (BAR) project [29]. The BAR project is focused on designing larger scale rotors and flexible blades capable of harnessing more wind energy while still navigating the transportation infrastructure within the United States. As part of the project a complete turbine was simulated including the tower, nacelle, hub, and blades. The BAR turbine assumed a 140 m hub height and 206 m rotor with a power rating from 150 W/m^2 (5 MW) [13,30], which this report scaled to 229 W/m^2 (7.5 MW) to better match California's moderate wind speeds.

The initial steel tower design was modeled entirely in NREL's Wind-Plant Integrated System Design and Engineering Model (WISDEM) [31], and was made to satisfy the DNVGL RP-C202 design code. An ASTM A572 Grade 50 Steel with a density of 7800 kg/m^3 was used in the simulations. The program and design were set to minimize the tower's mass, by constraining ultimate stresses, global (column) and shell (plate) buckling with a 1.1 safety factor, minimum diameter-to-thickness ratio of 120, bounds on max diameter of 6 m, max taper ratio of 0.2, and tower frequency that satisfies the soft-stiff configuration (soft-soft configurations were also examined, but could not satisfy all constraints with any of the diameter limits). Within WISDEM the design was tested against wind load cases to determine the loading factors used to calculate the structural stresses and necessary design adjustments. To approximate accurate wind loads, WISDEM will simulate steady-state "gust" cases with wind speed data taken from the peak of the Mexican hat from the IEC 61400 standards. To estimate the loads the wind causes due to the nacelle and blades the pitch and rpm are set as rated (the specific software load path involves transferring the WISDEM loads to the rotor, modeled in RotorSE, to DriveSE, and finally to the TowerSE, all open-source programs within the NREL family of public wind programs). These load cases are known to be conservative and are used to quickly estimate ultimate loads. Seismic and fatigue loads were not considered when designing this initial tower due to limitations within the WISDEM software when the original design was first built. The design loads for the steel tower are listed in Table 2.

Table 2 - 7.5 MW Steel tower design loads.

Design Loads (kN-m, unfactored)	7.5 MW 140 m Steel tower
Turbine Wind Moment	251,800
Direct Wind Moment (due to wind on tower)	83,804
Total Wind Moment	355,604

The WISDEM BAR tower design was idealized within OpenFAST as a continuously tapered unit to improve convergence in beam models, however this continuous tapering is inconsistent with current manufacturing practices for steel towers. For the purposes of this study the tower was split into sections (Figure 4) based on current industry design practices. To achieve this standard every tower section except the top section is cylindrical with a constant steel thickness; this setup is preferred in manufacturing due to the difficulty in rolling trapezoidal large-scale sections, versus the simpler rectangular sheets used for cylinders. The top section alone is designed to allow a slight taper, with a smaller upper radius compared to its base. This is because the highest section is subjected to the lowest loads and requires a lower steel thickness, which makes it easier to construct in comparison to the thicker lower sections. The top section is also traditionally the tallest section due to the aforementioned lower loads, as well as lower overall radius; this trend is apparent in many of the industrial towers built today by corporations such as GE, Goldwind, and Enercon. The modified tower sections are listed in Table 3. Because life-cycle assessment depends on inventory, adjusting the tower in such a way that the mass is maintained will still produce accurate life-cycle results for the original design, while also allotting for the calculation of the additional inventory features of flanges and bolts, which require both the number of sections and specific radii to accurately predict. While it is possible that there would be a change in tower mass based on this modelling design change, the BAR tower was designed with

conservative loads making it unlikely the mass would increase, and ensuring the LCA results therein remain accurate.

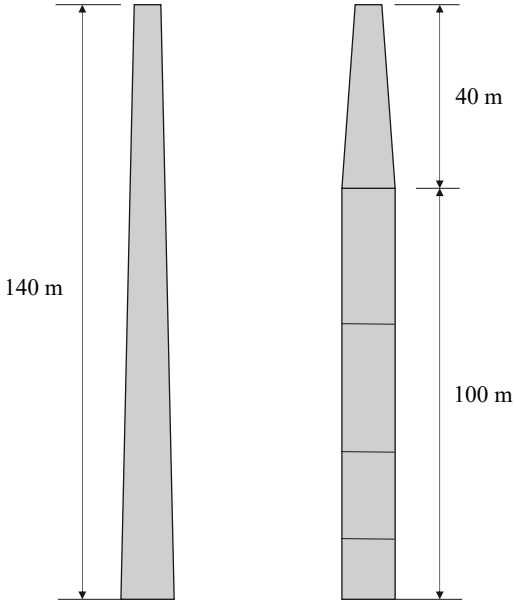

Figure 4 – Conversion from idealized tapered geometry to typical manufacturable sections.

Table 3 – Steel Tower individual section results for a 5-section tower. Top section is tapered, all others are static hollow cylinders. 7800 kg/m^3 steel density assumed.

Section Height (m)	**Total Height (m)**	**Thickness (m)**	**External Dia. (m)**	**Volume (m^3)**	**Mass (kg)**
12	12	0.05	6	11.215	87480.789
20	32	0.05	6	18.692	145801.315
32	64	0.045	6	26.940	210130.326
36	100	0.03	6	20.256	157994.716
40	140	0.0185	5.53	17.549	136884.237
			Total	94.653	738291.383

The second and third types of ultra-tall wind turbine tower considered in this study are reinforced concrete towers designed utilizing concrete additive manufacturing. The second type,

referred to as the On-site design, is designed with tower sections that are additively manufactured and assembled at the final tower erection site. Two variations of On-site design were considered, one using high strength (78 MPa / 11 ksi) printed cement, the second using a more typical strength (35 MPa / 5 ksi) printed cement. The third type, referred to as the Off-site design, is a reinforced concrete tower with a similar structural design as the On-site tower, but with the construction of the concrete sections taking part in two locations, with shells additively manufactured in offsite plants, which are then transported to the erection sites and assembled onsite. The 140 m reinforced concrete tower was designed based on ACI-318 and ACI-ITG-9R-16 to support a rated wind speed of 9.8 m/s with a maximum shear of 1,335 kN service load including dead load, direct wind load, and wind-induced turbine load. Seismic loads were also considered based on AWEA RP2011 load combinations and response-spectrum analyses conducted in LARSA-4D software, with ultimate moment capacity being computed using a non-linear strain-compatibility methodology in the XTRACT software.

Furthermore, this study assumed that all three types of wind turbines contain identical features in areas besides the towers, such as the design and geometry of foundations, nacelle, blades, and internal features i.e., stairs, elevators, gantry work, as well as initial site preparations. It is expected that the additively manufactured concrete tower can have different foundation designs than the steel towers, due to the differences in the weight, geometry, and structural behavior of the superstructure, and the geotechnical conditions specific to the tower sites; however, these can be considered in a future study.

2.3 Life Cycle Assumptions

The life cycle assessment framework considers five stages of the wind turbine structure's life cycle: (1) material production, (2) transportation, (3) manufacturing, (4) use, and (5) end of life. A service life of 25 years was considered, based on conservative design estimates chosen to maximize the lifetime of larger-scale turbines, as well as an acknowledgement of the advancement in technology since the early 2010s turbines with their projected 20-year service life. One benefit of conservative tower design is the possibility of replacing the hub as higher rated generators are developed while maintaining the original tower, encouraging a longer service-life tower design.

The case studies considered in this report are all of 140 m 7.5 MW towers, and include: (i) On-site 3D printed towers (35 MPa and 78 MPa), (ii) an Off-site 3D printed tower, and (iii) a standard tubular steel tower.

On-site refers to the tower sections being additively manufactured and assembled at the tower erection site. The proposed method would involve setting up a series of large-scale industrial 3D printers, that would use locally-supplied cement mixtures to construct each section in staging areas that the tower crane could reach and assemble after curing. Hoop reinforcement would be manually added during printing, and after print completion vertical reinforcement and post tensioning (PT) ducts would be inserted in designated block-out holes. Match casting would be used to ensure individual sections align properly during stacking and assembly. During stacking, 1 cm of connecting grout would be applied between sections to help affix them to one another. After stacking, post-tension strands will be lowered through the PT ducts and stressed at designated heights based on design. Finally, the PT ducts will be filled with grout, and the protection caps for the PT anchors will be installed and grouted. The design results for both On-site towers are summarized in Table 4.

Table 4 - Design results for On-site 3DCP tower.

Design results for On-site 3DCP tower.		**7.5 MW 140 m**	
3D Printed Concrete Strength		78 MPa	35 MPa
External diameter (mm)/thickness(mm)	Bottom Top	12200/762 3840/406	12200/914 3840/406
Volume of 3D printed concrete (m^3)		1928	2301
Volume of ready-mix concrete (m^3)		0	0
Volume of 55 MPa post-tensioning grout (m^3)		273	270
Mass of pre-stressing steel: 23-strand 270 Grade tendons (Metric ton)		138	138
Mass of #4 and #7 rebar (Metric ton)		227	227

3D printed concrete has a different rheology and material make up to standard cast-in-place concrete, as it must be liquid enough to extrude properly but stiff enough that once placed, it can hold its shape and not deform as more material is placed on top of it. This commonly results in 3DCP mixtures containing a higher volume of cement by weight than conventional concretes. However, some printable concretes are able to offset the high cement volume using cement mixtures like CEM2 that include mixtures of fly ash, as well as smaller gravels that will fit through printer hoses and nozzles. Table 5 lists the mix design used for the 78 MPa On-site tower design as well as the Off-site tower design considered in this report. Table 6 lists the lower-cement mix design used for the 35 MPa On-site tower.

Table 5 – 78 MPa 3D printed concrete mix design.

Material	Mass (kg/m^3)
Portland Cement	1002
Silica Fume	177
Sand	590
Water	312
Superplasticizer	17
VMA	0.6
Retarder	1

Table 6 - 35 MPa 3D printed concrete mix design.

Material	Mass (kg/m^3)
Portland Cement	338
Fly Ash	113
Sand	780
10 mm Gravel	880
Water	200
Superplasticizer	5
Stiffener	1.5
Accelerator	4.6

For the Off-site construction, only the external formwork of the sections would be printed, and those voids would be filled with standard cast in-place concrete prior to erection. In the Off-site pre-casting plant, 12 m stay-in-place segments would be printed with 78 MPa concrete using horizontal and vertical match casting, with each segment forming a partial arc that will be bolted or welded to one another in sets of six or four to form a complete cylindrical section; six arcs for the seven tower sections below 84 m and four arcs for the remaining five sections. Once the shell is printed vertical reinforcement and PT ducts will be installed, and select voids will be filled with standard concrete for stability during transportation. For this study locally sourced 35 MPa (5 ksi) pour-in-place concrete from CalPortland was assumed for all concrete aside from the 3D printed concrete. Post-curing, the segments will be transported to the build site and the cylindrical sections will be joined by 1 cm of connecting grout and bolting or welding the vertical joints of the arcs together, after which the final hollow voids will be filled with more cast-in-place concrete. The final steps are the same as the On-site process, including stacking, post-tensioning, and grouting prior to turbine and blade installation. Table 7 lists the design results used for calculating the LCA inventory for the Off-site tower.

Table 7 - Design results for Off-site 3DCP tower.

Design results for Off-site 3DCP tower.	**7.5 MW 140 m**	
External diameter (mm)	Bottom	12200
	Top	3650
Thickness (mm)	Bottom	914
	Top	406
Volume of 3D printed concrete (m^3)		1025
Volume of ready-mix concrete (m^3)		1574
Volume of 55MPa post-tensioning grout (m^3)		122
Mass of pre-stressing steel: 23-strand 270 Grade tendons (Metric ton)		137.89
Mass of #4 and #7 rebar (Metric ton)		226.796

The emissions values for the Southern California cast-in-place or "ready-mix" concrete were taken from the CalPortland Company's release of an Environmental Product Declaration in 2020 summarizing their LCA results for 30 Ready Mix Concrete mixtures from eight southern California plants [32]. These LCA results were calculated based on the US EPA Tool for the Reduction and Assessment of Chemical and Other Environmental Impacts (TRACI), version 2.1, 2012 impact categories. From these collected data, the eleven mix designs with strengths of 35 MPa (5000psi) were averaged to create a general value of expected concrete emissions in southern California. These averages included four of the CalPortland plants that were closest to Palm Springs: Alameda, El Segundo, LAX, and Normandie.

While the average presented a generally homogenous view of the concrete mixtures as a whole, the ADPfossil impact category (ADPf and ADPe) had a disproportionately large standard deviation compared to the other impact categories. This was determined to be because four of the eleven mix designs had a marked increase in that category alone, with values of roughly 2000 MJ, while the remaining seven had values near zero. To avoid an inaccurate average the singular mix design 45EF6Z was selected, due to its averaged impact indicator values being very close to the

net average of all the reported cements. Both the average and the 45EF6Z mix designs are listed in Table 8.

Table 8 – LCA emissions results for 1 kg of 35 MP (5000 psi) CalPortland ready-mix concrete sourced from the Los Angeles basin area.

Core Mandatory Impact Indicator			**Ready-mixed Concrete**	
		Units	Average	45EF6Z
Global Warming Potential	GWP	kg CO_2e	363.357	361.345
Depletion potential of the stratospheric ozone layer	ODP	kg CFC-11e	8.19E-06	6.79E-06
Acidification potential of soil and water sources	AP	kg SO_2e	1.49	1.17
Eutrophication potential	EP	kg Ne	0.122	0.120
Photochemical smog creation potential	POCP	kg O_3e	28.81	22.39
Abiotic depletion potential (ADPfossil) for fossil resources	ADPf	MJ, NCV	2891.96	2835.58
	ADPe		732.73	1.18E-04
Fossil fuel depletion	FFD	MJ Surplus	232.98	236.49

After determining the total impacts, the data was uploaded into the SimaPro simulation software in two different ways. In the first, the impact categories were recreated directly as generalized material outputs using the standardized units reported in TRACI. The second method was to adjust the closest existing SimaPro concrete mix design to match the impact emissions of 45EF6Z; the "50Mpa Concrete {GLO}| market for" material was selected for this purpose based on its GWP value of 369 kg CO_2e per m^3. The benefit of adjusting an existing material in SimaPro is that the unreported impact categories left out of the EPA report are also estimated appropriately within the simulation. However, since this study focused on six of the impact categories included in the CalPortland report (Tables 1, 8), this adjusted material was ultimately unneeded and the simplified direct approach was used.

The steel tower design was adapted from the "BAR: Big Adaptive Rotor Project", with technical data taken from NREL's GitHub BAR_USC design. As summarized in Section 2.2, since the original BAR tower was created as an idealized tapered model, the geometry was marginally adjusted to be more suitable for manufacturing and material inventorying, i.e., a single tapered tower was replaced with cylindrical sections and a tapered top (Figure 4), while maintaining the original tower mass. Exact tower details are listed in Table 9.

Additional design features such as flange volumes and bolt weights were extrapolated from existing industrial data trends and applied to the BAR design. Because flange mass depends primarily on section diameters, general trends are suitable to predict generic flange heights and depths; detailed estimates of flange and bolt masses are listed in Table 10. As this tower has a diameter greater than 4.3 meters, it was assumed to be built in 4 arcs per section for transit, and then assembled onsite using bolted flange connections. For simplicity these vertical flanges used the same flange designs and bolt ratios as the top of their respective section (i.e. For the tower base, an F2 flange was used on the vertical sides of the four individual pieces making up the section as well as on the top of the section). The exception to this rule was the top section, which used F5 flanges for the conjoining arcs as the F6 flange is a specialty flange meant to accommodate the hub of the tower.

Finally, the steel tower inventory includes a topcoat of epoxy paint on its exterior and an epoxy paint primer on both its exterior and interior surface; because the towers are onshore and not close to the ocean, a single coating was assumed. The total exterior surface area to be covered was 2609 m^2, and an interior surface area of 2577 m^2. For these coatings HEMPADUR 4774D was chosen for the primer material and HEMPATHANE HS 5561B was selected as the topcoat. An estimated material makeup for both coatings was extrapolated from the public safety data

sheets and recreated within the life cycle assessment software. The full list of paint process inventory is listed in Appendix A.

Table 9 - Design results for steel tower.

Design results for steel tower.	**7.5 MW 140 m**	
External diameter (mm)/thickness(mm)	Bottom Top	6000/50 5530/18.5
Mass of tower sections minus outfitting (Metric ton)		738.3
Mass of flanges (Metric ton)		152.2
Bolts (Metric ton/Number)		23.2/3749

Table 10 - Flange mass calculations. 7800 kg/m^3 steel density assumed.

Flange ID	**Diameter (mm)**	**Height (mm)**	**Neck Thk (mm)**	**Weight (kg)**	**Bolt Circle Dia. (mm)**	**Hole Dia. (mm)**	**No. of Holes**	**Volume (m^3)**
T Flange	6250	140	56	7656	5750	45	140	0.982
F2 Flange*	6000	161	31	4835	5804	67	132	0.620
F3 Flange*	6000	140	24	3232	5850	51	174	0.414
F4 Flange*	6000	120	20	2499	5870	45	150	0.320
F5 Flange*	6000	110	16	2254	5878	45	120	0.289
F6 Flange	5530	480	45	8555	5290	39	228	1.097
			Total	41854			Total	5.366

*Values doubled for the total since flanges are used twice for the top/bottom of interior section connections.

In addition to the general tower design, a detailed scenario was constructed to calculate the time and distance traveled for components of the manufacturing process, summarized in Table 11. San Gorgonio near Palm Springs, California, was selected as the target tower site location, based on its current wind power capacity as well as its proximity to industrial and staffing locations. This location was used to calculate the total distances traveled by the tower components in the LCA model. For the concrete sections, the precast location used for the Off-site tower was a local concrete plant 100 km from the build site, the ready mix plant used for the On-site towers was a

local ready mix plant 6.5 km from the build site, and for the steel tower sections the CS Wind plant in Pueblo, CO, 1,627 km from the build site was used. To calculate the proper emissions of the coatings, the Hempel plant in Northlake, TX, located 1,027 km from the steel manufacturing site, was selected.

The number of sections in each proposed tower was also taken into account so that the most accurate erection time per tower could be modeled, based on the assumption of 1 section mounted per hour of crane time for both concrete and steel sections. This mounting time is optimistic based on tower mounting times that can take 2 to 3 hours per section, but is simplified as it assumes the crane is running for a full hour rather than idling at any stage during production. A Liebherr LR 11000 crawler crane was used in the model for this purpose based on its load capacity and height limits. The crane operates using a 500 kW (680 hp) diesel engine [33], which corresponds to a steady-state load based on EPA emissions guidelines in NR-005d [34]. Based on these criteria the appropriate SimaPro database was selected to calculate emissions (Machine operation, diesel, >=74.57 kW, steady-state).

Table 11 - LCA transportation and construction variables.

General		
	Tower location	San Gorgonio, near Palm Springs CA
	Worker travel distance (km)	11.3
	Workers during crane assembly	150
	Workers during other assembly	20
Concrete		
	Precast location	Clark Pacific (13592 Slover Ave, Fontana, CA 92337)
	Distance from plant to tower (km)	100
	Ready-mix location	Robertson's Ready Mix (13990 Apache Trail, Cabazon, CA 92230)
	Distance from ready-mix to tower (km)	6.5
On-site		

	Number of sections	46
	Height of sections (m)	3
Off-site		
	Number of sections	12
	Height of sections (m)	12
Steel		
	Section manufacture location	CS Wind (100 Tower Rd, Pueblo, CO 81004)
	Distance from plant to tower (km)	1,627
	Coating manufacture location	Hempel (4201 Dale Earnhardt Blvd, Northlake, TX 76262)
	Dist. From paint to steel plant (km)	1,027
	Number of sections	5
	Max section height (m)	38
	Min section height (m)	12

During the use phase, a 25-year service life is considered, with a manual inspection taking place three times a year. For wind turbines, the towers themselves are subjected to minimal maintenance over the lifetime of the unit. During steel tower maintenance the primary tower checks are bolt tension and ensuring the tower coating is undamaged to avoid steel corrosion. This study considered a scenario where 5% of the steel tower would be recoated with primer and topcoat on an annual basis over the course of the tower's total lifespan (modern coating warranties can easily extend to 20 years making this a probable overestimate of the maintenance). Concrete towers require even less scheduled maintenance, as they do not require a painted coating, leaving just the triannual inspection of the post tensioning strands and other visual maintenance.

After 25 years, the end of life phase considers both recycling and landfill scenarios. For the concrete towers, the landfill scenario considers demolition of the tower, and transit of the waste mass to a local inert landfill. This is the traditional fate of most concrete structures, however there has been increasing interest in developing methods to reuse old concrete to reduce the environmental impact of that material. One proposed method of recycling concrete structures is to

break the concrete down into aggregate which can be used locally for road infrastructure. To account for this potential end of life a recycling scenario sets aside 70% of the concrete and steel reinforcement as being considered recycled. In this scenario the total mass of the concrete tower that is not recycled is considered waste and would be transported to a local inert landfill. For the steel tower, a steel recycling rate of 90% efficiency was considered in the body with 70% for the flanges and bolts, with the remainder being sent to a landfill. In this instance the reclaimed steel would be transported to a local recycling plant for eventual reuse. The distance from the turbine field to the recycling plant was considered to be 34 km, and the distance from the turbine field to the landfill was considered to be 24 km for all materials.

To account for the environmental offset of recycling materials, this report assumes that the recycled material replaces the corresponding virgin material in the initial tower construction. In terms of calculating LCA emissions this means that the total volume of material being measured is the difference between the initial material content and the equivalent recycled content. For steel the recycled component is measured as scrap steel and replaces that ingredient in the tower construction phase. For concrete, the concrete waste is recycled as crushed aggregate to offset the initial aggregate component of the concrete. It is also assumed that the concrete waste must crushed prior to being recycled. In this study a Screen Machine 5256T Impact Crusher with a 354 kw diesel engine, recorded as steady-state within SimaPro based on EPA regulations, was modeled using a 1 m^3 per minute crushing rate.

Within the specifics of the simulation the exact percentages of scrap material utilized are unlisted. The steel tower was simulated using the steel welded pipe material component within SimaPro. This material was selected due to its inclusion of cylindrical bending processes that are also present in tower construction. For calculation purposes the virgin steel that was offset by the

recycled tower was calculated within the software as iron pellets rather than rolled steel pipe, in order to not undercount the steel treatment and processing taking place. The rolled steel pipes are made of thinner sheets and therefore a BOF steel mill was considered for the tower body, while EAF processing was considered for the steel reinforcement (rebar, post tensioning, nuts, bolts) [35]. BOF steel mills produce steels with less contaminants but as such also use a lower percentage of scrap steel. The tower body was assumed to contain 30% scrap steel by volume while the reinforcement was assumed to contain 90% scrap by volume [36].

3. Simulation Results

The inventory analysis carried out for each design was transposed into the life cycle assessment software SimaPro, ver. 9.0.0, which was used to carry out emissions calculations using the Environmental Protection Agency's Tool for Reduction and Assessment of Chemicals and Other Environmental Impacts (TRACI 2.1 V1.05/ US 2008) analysis framework. The first model calculates the total sum of the transportation, materials, construction, use, and end of life costs for each tower using the six impact assessment categories from Table 1, displayed in Figure 5. Based on these initial data the steel tower has the lowest impact in ozone depletion, eutrophication, and fossil fuel depletion, while the 35 MPa On-site tower has the lowest global warming, smog, and acidification emissions. These towers are followed by the Off-site tower and finally the 78 MPa On-site tower, which has the highest emissions in all six categories by a notable margin. To fully

understand the nature of these findings the total values were broken down into Table 12 by their relevant life cycle categories: transportation, materials, construction, use, and end of life.

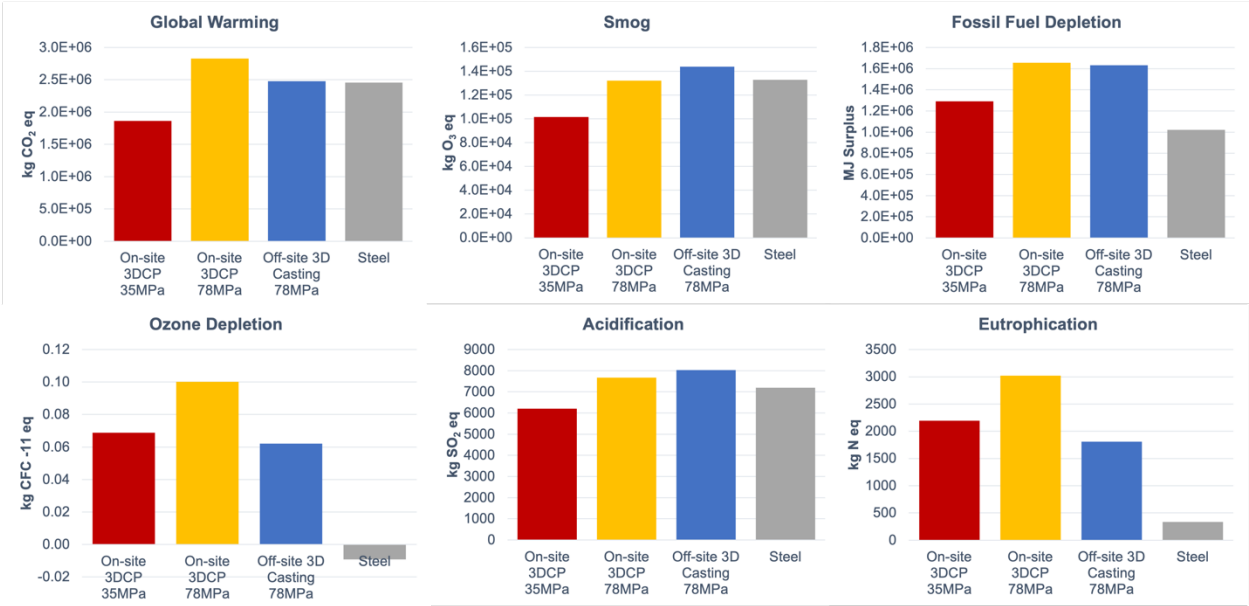

Figure 5 - Total life cycle emissions using TRACI analysis of 35 MPa On-site, 78 MPa On-site, Off-site, and Steel wind turbine towers.

Table 12 - Summarized impacts of 35 MPa On-site, 78 MPa On-site, Off-site, and Steel wind turbine towers broken down by life cycle stage contributions.

	Ozone depletion	Global warming	Smog	Acidification	Eutrophication	Fossil fuel depletion
On-site 35MPa	kg CFC-11 eq	kg CO_2 eq	kg O_3 eq	kg SO_2 eq	kg N eq	MJ surplus
Transport	4.63E-07	11063	3260	129	8	23243
Materials	**6.53E-02**	**1830308**	**92341**	**5923**	**2275**	**1163244**
Construction	8.92E-04	14654	1930	82	7	30789
Use	3.84E-08	926	113	5	0.3	1927
End of Life	2.65E-03	5724	3935	72	-97	72326
Total	6.88E-02	1862674	101579	6210	2193	1291529
On-site 78MPa	kg CFC-11 eq	kg CO_2 eq	kg O_3 eq	kg SO_2 eq	kg N eq	MJ surplus
Transport	4.23E-07	10109	2979	118	7	21239
Materials	**9.66E-02**	**2794524**	**123747**	**7420**	**3082**	**1538197**
Construction	8.92E-04	14654	1930	82	7	30789
Use	3.84E-08	926	113	5	0.3	1927
End of Life	2.61E-03	7290	3258	55	-75	62952
Total	1.00E-01	2827503	132027	7679	3021	1655104
Off-site	kg CFC-11 eq	kg CO_2 eq	kg O_3 eq	kg SO_2 eq	kg N eq	MJ surplus
Transport	3.20E-06	76450	22519	889	53	160621
Materials	**5.94E-02**	**2387158**	**116277**	**7026**	**1843**	**1385630**
Construction	2.33E-04	8174	1047	46	3	17109
Use	3.84E-08	926	113	5	0.3	1927
End of Life	2.39E-03	4136	3822	70	-91	67413
Total	6.21E-02	2476844	143777	8036	1809	1632701
Steel	kg CFC-11 eq	kg CO_2 eq	kg O_3 eq	kg SO_2 eq	kg N eq	MJ surplus
Transport	2.54E-05	143315	49176	1910	115	300791
Materials	**-7.69E-03**	**2320082**	**86118**	**5440**	**296**	**711159**
Construction	7.78E-05	6209	762	34	2	12943
Use	8.46E-04	9149	704	50	34	16203
End of Life	-2.37E-03	-24515	-3827	-234	-112	-19033
Total	-9.12E-03	2454239	132933	7201	335	1022063

Note: Maximum values in each category are in bold.

As expected in terms of transport, the steel tower's transport emissions are greater than both the On and Off-site printed towers because of the additional distance the steel sections had to travel to reach the build site in comparison to the concrete components. This difference is likely an underestimate as well, as this model did not take into account the emissions from the two transport vehicles required by law to escort each tower segment. In addition, the On-site transportation is lower than the Off-site due to the materials only having to travel from a nearby ready-mix site

rather than the slightly farther prefabrication plant. However, in terms of the construction stage the towers begin to show different trends. While steel has less construction emissions than both concrete towers, the Off-site tower has approximately half of the emissions of the On-site towers. This can be explained by examining which parts of the life cycle model are categorized as construction contributions, namely the daily transit of the workers to the build site, and the crane used to assemble the towers (as all other construction features are considered to be identical for all towers and are not simulated). While the difference between the volume of workers and their daily commute between the four towers was minimal, the amount of crane time for each design varied dramatically, and in fact was observed to be the largest contributor to the construction stage of the model. The difference in the construction costs of each tower can be tied almost precisely to the number of hours, and by extension the number of sections, that the crane was operating on. The steel tower with its 5 sections is the lowest, followed by the 12 section Off-site tower, and capped by the substantial 46 section On-site towers, which have emissions over three times the steel tower.

While the transit and construction stages of the life cycle assessment provide interesting results, the largest stage by far is the material contribution. When each process is broken down into percentage contribution of total in Table 13, the material category is the driving factor in each category, as illustrated further in Figure 6.

As such, while there is good measure in investigating the other life cycle stages such as developing improved transportation and construction practices for turbine towers, in terms of net lifetime emissions the materials stage is where any substantial improvements are likely to be made, in particular in the global warming category. Based on this breakdown a closer analysis of the

materials stage will determine what specific factors are driving the key differences in emissions between the three towers.

Table 13 - Life cycle stage contribution by percentage of total.

	Ozone depletion	Global warming	Smog	Acidification	Eutrophication	Fossil fuel depletion
On-site 35 MPa						
Transport	0.001%	0.6%	3.2%	2.1%	0.3%	1.8%
Materials	**94.9%**	**98.3%**	**90.9%**	**95.4%**	**95.3%**	**90.1%**
Construction	1.3%	0.8%	1.9%	1.3%	0.3%	2.4%
Use	0.00006%	0.05%	0.1%	0.1%	0.01%	0.1%
End of Life	3.9%	0.3%	3.9%	1.2%	-4.0%	5.6%
On-site 78 MPa						
Transport	0.0004%	0.4%	2.3%	1.5%	0.2%	1.3%
Materials	**96.5%**	**98.8%**	**93.7%**	**96.6%**	**97.2%**	**92.9%**
Construction	0.9%	0.5%	1.5%	1.1%	0.2%	1.9%
Use	0.00004%	0.03%	0.1%	0.1%	0.01%	0.1%
End of Life	2.6%	0.3%	2.5%	0.7%	-2.4%	3.8%
Off-site						
Transport	0.005%	3.1%	15.7%	11.1%	2.7%	9.8%
Materials	**95.8%**	**96.4%**	**80.9%**	**87.4%**	**92.6%**	**84.9%**
Construction	0.4%	0.3%	0.7%	0.6%	0.2%	1.0%
Use	0.00006%	0.04%	0.1%	0.1%	0.01%	0.1%
End of Life	3.9%	0.2%	2.7%	0.9%	-4.6%	4.1%
Steel						
Transport	0.2%	5.7%	35.0%	24.9%	20.6%	28.4%
Materials	**69.8%**	**92.7%**	**61.3%**	**70.9%**	**52.9%**	**67.1%**
Construction	0.7%	0.2%	0.5%	0.4%	0.4%	1.2%
Use	7.7%	0.4%	0.5%	0.7%	6.1%	1.5%
End of Life	-21.5%	-1.0%	-2.7%	-3.1%	-20.0%	-1.8%

Note: Maximum values in each category are in bold.

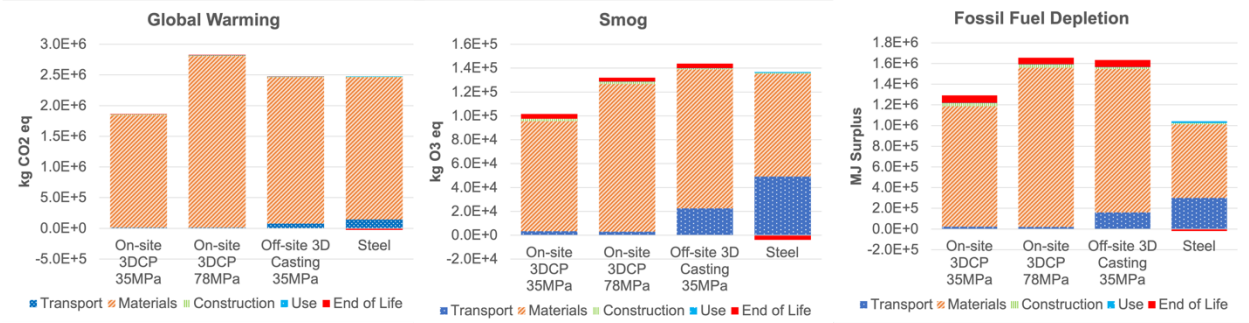

Figure 6 - Life cycle emissions results broken down by stage contribution.

The specific material breakdown in this report focuses on the material contributions of each tower in terms of Global Warming Potential. GWP is one of the largest emissions categories measured that directly contributes to climate change, and that also has the highest purely material contribution via Table 13: 92% and greater for each of the four towers. From the comparison of each tower in Figure 7 it's apparent that the primary contributor to the On-site tower's total emissions stems from the 3D printed concrete, as the two different mix designs for the 35 MPa and 78 MPa printed concrete produce substantially different emission results. Since the 35 MPa On-site design uses a printed mixture with less cement content and the Off-site design offsets its use of high percentage printed concrete with standard ready-mix concrete, the emissions are substantially lower. This indicates that the primary contribution to the high emissions of the concrete towers is the 3D printed concrete material.

As for the steel tower, the material of the body understandably makes up nearly all of the material contributions, with the smaller additions such as the bolts and paint having a minimal impact on the total emissions. The paint in particular is important to mention with respect to the "use" phase of the steel turbine. Even assuming a 5% annual repainted area, the net emissions from these maintenance actions are minimal, as quantified in Table 11. Another notable aspect of the steel tower breakdown is the material contribution of the flanges. Since the steel tower has a

6 m base diameter it requires segmentation for traditional transit, which is limited to 4.3 m, so each tower section is made of 4 arcs that are connected via additional bolted flanges. If the tower were constructed onsite using methods such as continuous welding, the emissions due to materials could be reduced by 2.05E+05 kg CO_2 equivalent. Note that this comparison does not take into account the additional environmental costs that this tower approach would incur, such as fabrication site preparation, which would be the focus of additional study.

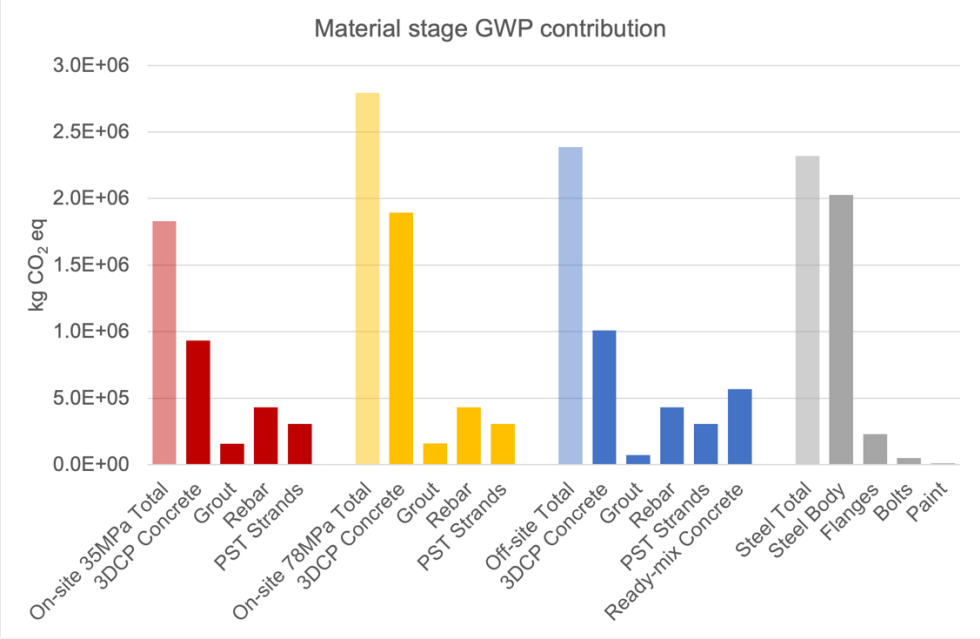

Figure 7 - Global Warming Potential of the three tower designs split by individual material contributions. From left to right: 35 MPa On-site tower, 78 MPa On-site tower, Off-site tower, steel tower.

Because of the perceived emissions difference between the 3D printed concrete and the conventional ready-mix concrete, the next set of simulations compares the two 3D printed concrete mix designs to the CalPortland conventional concrete. A summation of the first 3D printed concrete mix designs is listed in Table 5 and 6. SimaPro's material database was used to model

each component as closely as possible, and in cases where a one-to-one comparison material did not exist in the database, a similar component was selected. For exact details on these substitutions refer to Table A.3 in Appendix A. Silica Fume was not included in the simulated mix design to correctly represent the fact that that material is a recycled industrial waste byproduct, and therefore would not add to the emissions of the concrete mixture. A calculated analysis of 1 m^3 of the 78 MPa 3D printed concrete, with an assumed density of 2100 kg/m^3 derived from weighed lab samples of the same mix design, was carried out to determine which factors within the mix design had the highest impact on emissions, as well as to verify that the substituted components produced the expected results. Based on this analysis, the Portland cement had the largest environmental impact by a significant margin, as shown in Figure 8. The additional ingredients that make up the mix design have minor impacts on the total global warming potential of the material. This indicates that for future mix designs, so long as the relative percentage of Portland cement is reduced, the overall net emissions of the material will decrease respectively. This makes research options such

as increasing particulate size, or taking advantage of more recycled materials like silica fume or environmentally cheaper materials like sand, a promising approach for future 3DCP development.

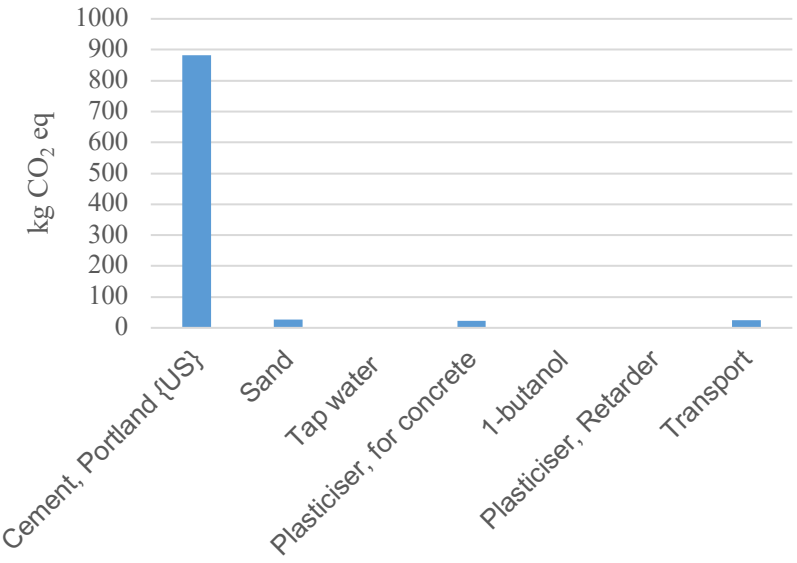

Figure 8 – Individual material environmental impact comparison for 1m^3 of the 78 MPa 3D Printing mix design. Transport was simulated based on SimaPro's existing market transit value of cement mixtures.

Comparing this 3D printed concrete mix design to the 35 MPa printed concrete as well as CalPortland averaged ready-mix concrete, the 78 MPa mixture has approximately three times the global warming potential, as seen in Figure 9. One factor contributing to this higher environmental cost is the size of the filler material; because the 78 MPa concrete does not use larger scale gravels, the ratio of cement per unit volume is higher than in conventional concrete. The shift from the conventional 13.48% and 14.54% cement by weight, for the CalPortland [37] and 35 MPa materials respectively, to 47.73% by weight in the 78 MPa mixture is a significant factor in the substantial emissions increase between the materials, and by extension the high observed emissions of the 78 MPa On-site concrete tower. (For the CalPortland concrete, the percentage of

cement by weight was extrapolated from EcoInvent 3's "Concrete, 35MPa {RoW}| concrete production 35MPa, RNA" mix design).

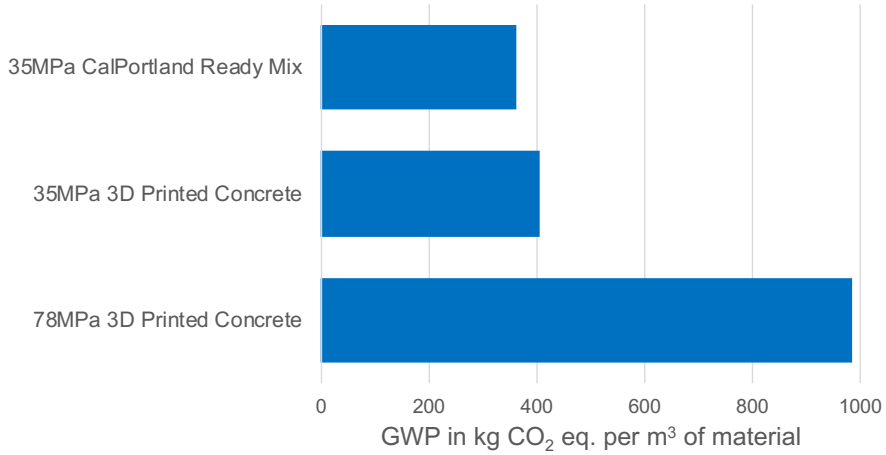

Figure 9 – 1 m^3 of conventional ready-mix concrete compared to 1 m^3 of 35 MPa (5 ksi) and 78 MPa (11 ksi) printed concrete in terms of Global Warming Potential.

From these observations, the next set of simulations compares the original 3D concrete printed and steel tower models to a concrete tower made purely out of conventional ready-mix concrete, replacing the 78 MPa 3D printed concrete material in the Off-site tower. Figure 10 helps to visualize the full impact of adjusting printed concrete in the tower designs by comparing the results of the printed towers to those of the new conventional concrete tower. Based on these initial findings, shifting to 78 MPa 3D printed concrete increases the global warming potential of the Off-site tower by approximately 45%. These findings also indicate that towers that fully utilize ready-mix concrete as their primary structural material do have a lower global warming potential than the matching steel tower. It is important to note that this simplified model does not include the emissions data for the formwork needed for a truly traditional cement tower and the total material

volumes are unchanged; instead, this graph is an indication on how a concrete tower would perform with the same construction process but different building materials.

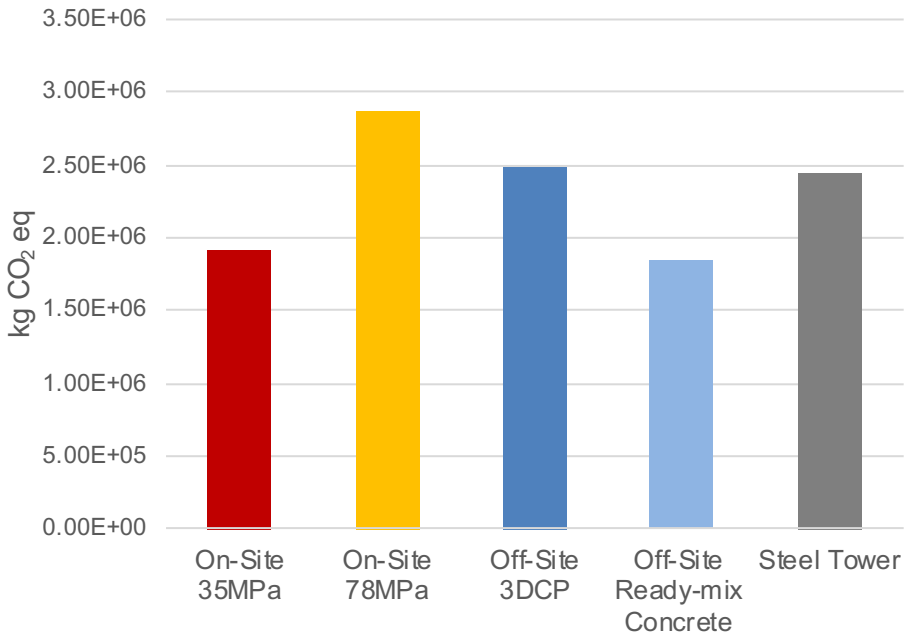

Figure 10 - 3D printed concrete towers compared to steel towers in terms of global warming potential, and then compared against an Off-site tower where the total concrete volume has been replaced with conventional ready-mix concrete.

From this data and the individual concrete emissions values in Figure 10 it is possible to calculate the total ratio of ready-mix to 3D printed concrete that would result in a cement tower with an equivalent global warming potential to the steel baseline tower using varying 3DCP mix designs. Through this strategy it is possible to predict what ratios of conventional to printed concrete would match an equivalent steel tower for unique 3D printed concrete mix designs. Similarly, current 3D printed mix to ready mix ratios can be adjusted to match lower emissions goalposts, such as those from a more conventional hybrid or welded steel tower.

As an example of this strategy, another lab-tested 3D printed concrete mix design was simulated within SimaPro using the same methods as the original. This design had a cement percentage by weight of 48.5% and a density of 2200 kg/m^3, a 0.7% and 5% increase respectively from the original 78 MPa mix design. While these adjustments were minor, their impacts on the cumulative tower emissions were significant. The default ratio of printed concrete to cast concrete for the original Off-site tower is approximately 2 to 3 (1025 m^3 to 1574 m^3 respectively). However, in order to match the GWP emissions of the steel tower with the new mix design, this ratio is instead approximately 1 to 2 (893.9 m^3 3DCP to 1705.02 m^3 ready mix). This accounts purely for the GWP of the material stage in production, and for the remaining impact categories the steel tower remains the lowest emitter, implying that more printed concrete must be reduced in order to match the steel tower for each environmental impact category.

The reduction of 3D printable material means that printing a full shell out of this new cementitious mixture may be difficult or impossible. Rather than printing a full perimeter for the sections, it is possible that this limited amount of material could be used to print key areas that would be difficult to construct via formwork, or that internal printing around the post tensioning gaps could be replaced with simple formwork rather than printed slots. Alternatively, shifting the design to incorporate the lower emission 35 MPa printable concrete, similar to what was done with the On-site tower, may allow the Off-site tower to lower its overall emissions while still using more printed material. This calculation once again indicates that smarter designs and green printable material development will be a key factor in making 3D concrete printed towers environmentally feasible.

4. Discussion

Based on these life cycle simulations, the 35 MPa On-site printed tower appears to be lower than a conventional steel tower of the same height and power rating in terms of global warming potential, although not in ozone depletion, eutrophication, and fossil fuel depletion. In addition, the differences between the printed tower scenarios, especially the 35 MPa and 78 MPa On-site towers, indicates that intelligent variation of concrete tower design that prioritizes less cement-dependent concretes can result in towers with vastly improved emissions. This improvement has the potential to be extended further by considering tower designs that take full advantage of 3D printing's greatest strength, its freedom of traditional design constraints. 3D printing has always been a realm that best serviced areas that cannot be produced via traditional means, as more often than not in a one-to-one comparison traditional means will be cheaper in terms of labor and materials used.

Investigating ways that 3D printing can reduce total material used can make the technology more of a contender against other proposed tall wind turbine technologies. Early photographs of GE's foray into 3D printed concrete wind turbine design show tower sections constructed with spacious infill, or empty space, between the inner and outer walls of the tower. This is one aspect of 3D printed design that has the potential to reduce materials and emissions. From the simulation results in this report, the Off-site tower saves printed material compared to the 78 MPa On-site tower by only printing the external shell of the tower, which drastically lowers the total tower emissions even though both designs are using a high strength/high cement content material. This indicates that for large scale concrete 3D printed structures that require high cement-content concrete, prioritizing total surface area as a design parameter may reduce emissions.

While one recycling scenario was considered for end of life, future research can be spent investigating other end of life scenarios such as refurbishing a tower to accommodate a new hub of greater or equal power rating, or a relocation of the towers. It is worth noting that the concrete towers were designed with seismic loads in mind, while the steel tower did not account for that additional load case. Concrete towers are more susceptible to seismic forces and a conservative overestimation was assumed when selecting the steel tower design, but this can be an oversimplified approach. Towers above 100 meters are generally governed by wind loading rather than seismic, but as seismic design can at times add up to 30% additional foundation or tower mass [16], confirming the results in this report against seismically loaded steel towers would ensure a more accurate method of comparison.

To that end while this report focused on a comparison to a conventionally designed steel tower, current industry trends point towards other styles as the more likely candidates for future construction. Concrete steel hybrid towers as well as novel approaches to singular material towers like continuously welded steel or Hexcrete concrete towers should be included in future life cycle studies of large scale onshore wind turbines that aim to capture a more realistic picture of the modern wind industry. Due to their lower material inventory, it can be reasonably expected that these towers will have notably lower emissions than the simplified steel tower considered in this design.

4.1 Parametric Study

To further expand upon the LCA results, each of the life cycle stages was individually analyzed using parameter variation with the goal of tracking relevant trends that can be used to make general predictions of future designs and processes. The individual variables selected for each life cycle stage are described in Table 14.

Table 14 - LCA stages parameter variables.

Life Cycle Stage	Varied Parameter
Transport	Distance of concrete plant to build site
Materials	% of cement by weight in printed concrete
Construction	Number of tower segments
Use	Rated tower life
End of Life	Tower recycling rate

The first stage considered was transportation. The transportation stage contains the transportation of the tower segments and relevant construction equipment from their originating sources to the final tower erection site, and the emissions of this stage with respect to GWP can be observed in Figure 11. For the steel tower all components are considered to have been transported from Pueblo, CO to the Palm Springs erection site, which is a constant value as it does not rely on the location of the concrete plant. Similarly, the On-site towers are built at the erection site with the concrete material being transported 6.5 km from a nearby ready-mix plant and are constant values, with the 35 MPa On-site tower having marginally higher emissions than the 78 MPa On-site tower due to its larger mass. The Off-site tower is constructed at the concrete fabrication plant 100 km away from the erection site, and is subject to the variance of that distance being increased or decreased. In addition, all of the concrete towers include the transportation of the 3D printers as well as the steel components, which were considered to be sourced from 148 km away in the Los

Angeles region. Because the Off-site tower requires materials to first be delivered to the concrete plant and then an additional distance to the erection site, the overall GWP emission from transport is higher than that of the On-site towers unless the precast location is less than 6.5 km away from the final erection site. Since the overall mass of concrete used in the Off-site tower is larger than that of the On-site towers, it requires a shorter total distance travelled in order to have a lower transportation stage emission. Based on this parametric study, the transportation emission benefits the concrete towers have over the steel tower from using locally sourced concrete becomes less viable as the distance between sites increases, and past 200 km the Off-site concrete tower will have larger transportation emissions than the steel tower. This approach can be used to validate site planning in the earlier stages of a project seeking to reduce transportation environmental costs.

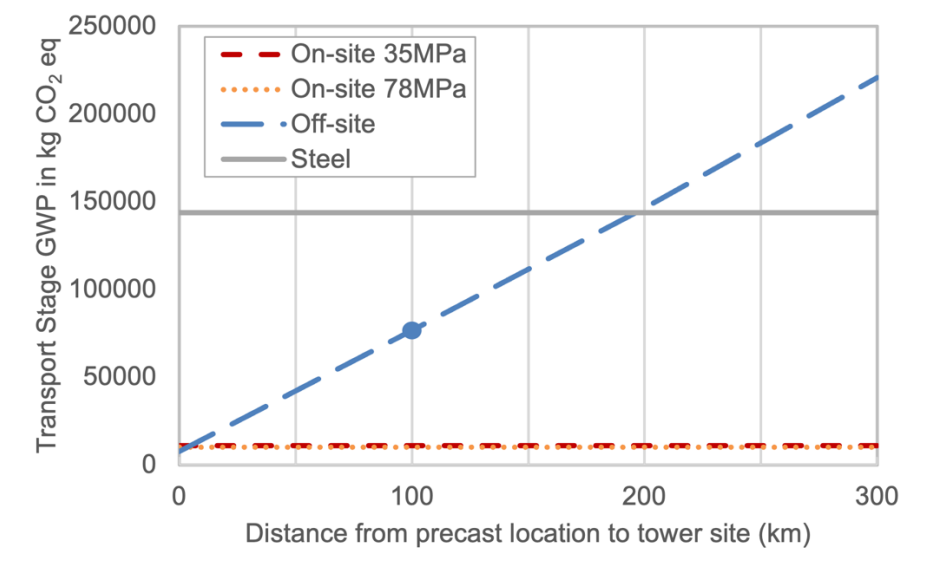

Figure 11 - Transportation stage parameter variation.

One point of note not considered in this analysis was the premise of imported steel towers. According to the 2021 Land-Based Wind Market Report, 25-40% of wind turbine towers in the United States are imported [38]. Adjusting the transportation stage from domestic road transit to

international freighting adds a significant amount of transportation stage emissions for the steel tower. For example, shipping the steel tower overseas from Hong Kong to Los Angeles results in a nearly 150% increase in the GWP of the transportation stage for the steel tower. In addition, imported foreign steel in domestic manufacturing can also play a role in overall materials emissions. The value of the emissions is dependent on both the origin country of the steel production and the type of steel manufacturing used, BOF or EAF [39], and is a complex subject worth investigating further in future studies, particularly those focusing on steel towers.

The next stage considered in the life cycle assessment is the materials stage. Since this stage makes up over 90% of the overall GWP emissions for each tower via Table 13, it is the most impactful of the stages and the area where the most dramatic shifts in overall emissions are likely to be made. Based on observations in the initial study, the percentage of cement in the printed concrete was identified as a driver of total emissions for the printed towers. This parameter variation expanded upon this by recalculating the emissions results of the material stage for each tower with a varied percentage of cement by weight in the printed material. This was a simplified substitution that did not account for the change in density of the new materials, and simply offset the original mix designs with new designs that preserved the ratio between other concrete ingredients while reducing the percentage by weight of cement. As seen in Figure 12, the varied slopes for each tower are indicative of the total mass of the printed cement in each design. The more printed material there is, the more the cement content by mass will impact the overall GWP emissions. Each design's trend line also indicates the point at which the designs become viable compared to the steel tower, as seen where the two lines intercept. For instance, for the 78 MPa On-site tower to match the material emissions of the steel tower with the same volume of material, the percentage by weight of the cement in the printed material must be reduced by slightly over

10%, from 47.73% by weight to 34.8% by weight. From here the new mix design would have to have its strength checked and if it is lower, the overall tower design may need to be reworked for that lower strength concrete. Alternatively, the total volume of printed concrete can be reduced, similar to making a cement shell design like the Off-site tower. This check and rework strategy is similar to existing structural design trends, as well as being the general premise behind computer automated generative design, and can be added in as another design variable during initial structural planning. This strategy can be adopted for future projects to predict what volumes and/or masses of printed material can be utilized in a design to reach specific emissions goals.

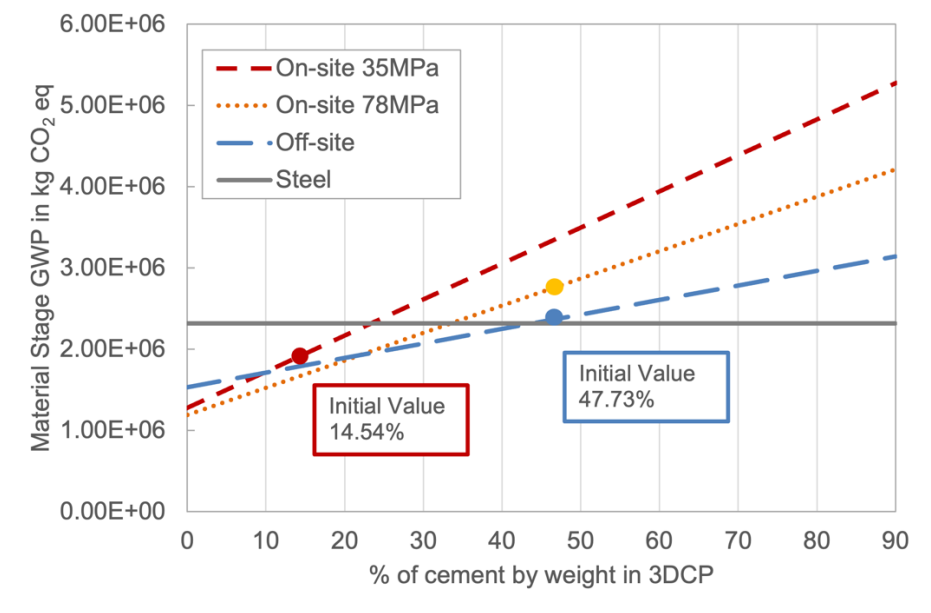

Figure 12 – Material stage parameter variation.

The construction stage of the life cycle assessment includes the transportation for workers to and from the build sites, as well as the machine operation of the crane and 3D printers. Of these contributing factors the run time of the crane had proportionally the largest impact on the construction stage. Because the crane run time is tied directly to the number of tower sections,

varying the tower sections was the variable focused on in the construction stage parametric study, seen in Figure 13. As the crane run time is assumed to be identical for all individual sections, steel and concrete, the slopes for each tower are identical. The differences in initial values are a result of the number of workers/distance traveled, as well as the length of run time for the 3D printers. As the On-site towers use the same number of workers and hours of printing, they are combined into one common trend line. Since there are no interceptions a direct comparison between the four towers is less profound; instead this parameter variation simply reemphasizes the impact section quantity has on GWP, as a measurement of overall construction time.

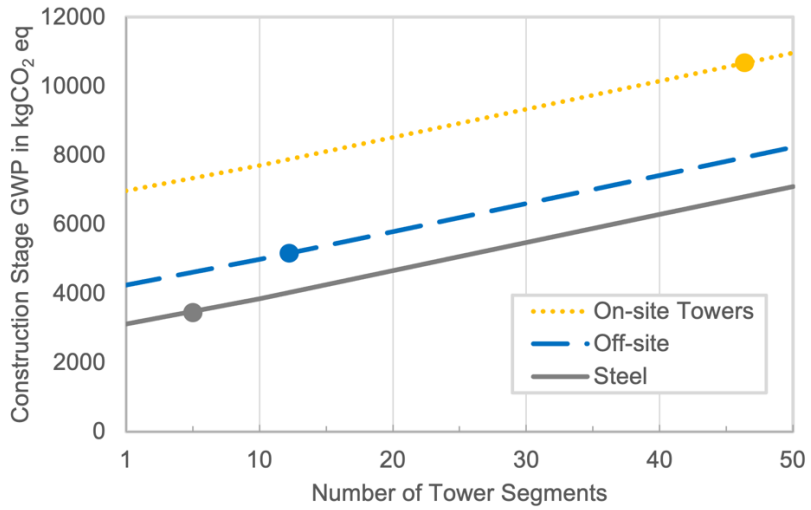

Figure 13 - Construction stage parameter variation. Initial values for the report indicated with focused points.

The use stage had the smallest number of variables contributing to it and is comprised solely of the transportation to and from the site of the maintenance team, and in the case of the steel tower a presumed 5% replacement of the painted coating every year. While the increase in

rated tower life does lead to a more marked increase in emissions for the steel tower than the concrete tower as seen in Figure 14, the total use stage emissions of a 100 year rated steel tower would only be 1.4% of its overall GWP emissions. This indicates that should the designs be made to a higher lifetime rating, the overall life cycle emissions would not see any significant changes.

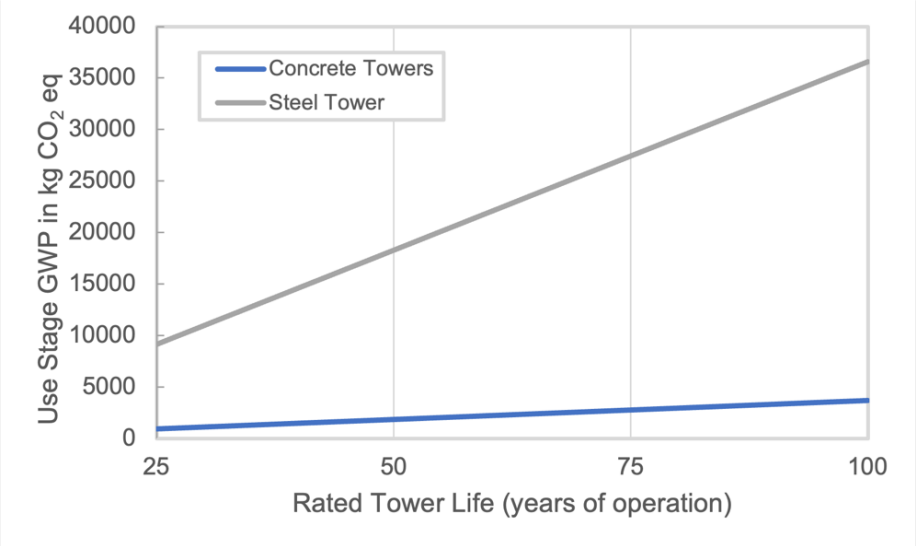

Figure 14 - Use stage parameter variation.

The end of life stage of the life cycle assessment includes the deconstruction of the towers, including crane operation and worker transportation, material crushing for the concrete towers, and transportation from the tower site to the recycling plant or inert landfill. The landfill was presumed to be located 24 km from the tower site and the recycling plant 34 km from the tower site. For the cement towers, a concrete crusher operating at 1 m^3 per minute using a 354 kw diesel engine was modeled within SimaPro. For the original parametric study all concrete tower components had a 70% recycling rate, while the steel tower had a 90% recycling rate for the body and a 70% recycling rate of the flanges and bolts. For the recycled material to be

properly credited within the LCA, the material that was recycled was considered an offset of the original content of recycled material within the towers. For the concrete this material was offset as aggregate gravel. The CalPortland ready mix used 41.04% gravel by weight and the 35 MPa printed concrete mixture used 37.91% gravel by weight, while the 78 MPa printed concrete used no gravel additives. Applying these recycling rates to the overall weight of the concrete used in each tower, the Off-site tower uses 24.66% recycled aggregate, the 35 MPa On-site tower uses 34.12% recycled aggregate, and the 78 MPa On-site tower uses no recycled aggregate. For all the steel components of the concrete towers it is assumed that the steel is comprised of 90% recycled material. For the steel tower, it is assumed that the tower body is made using BOF steel production and includes 30% recycled material by volume, and the flanges and bolts are made using EAF steel production using 90% recycled material by volume.

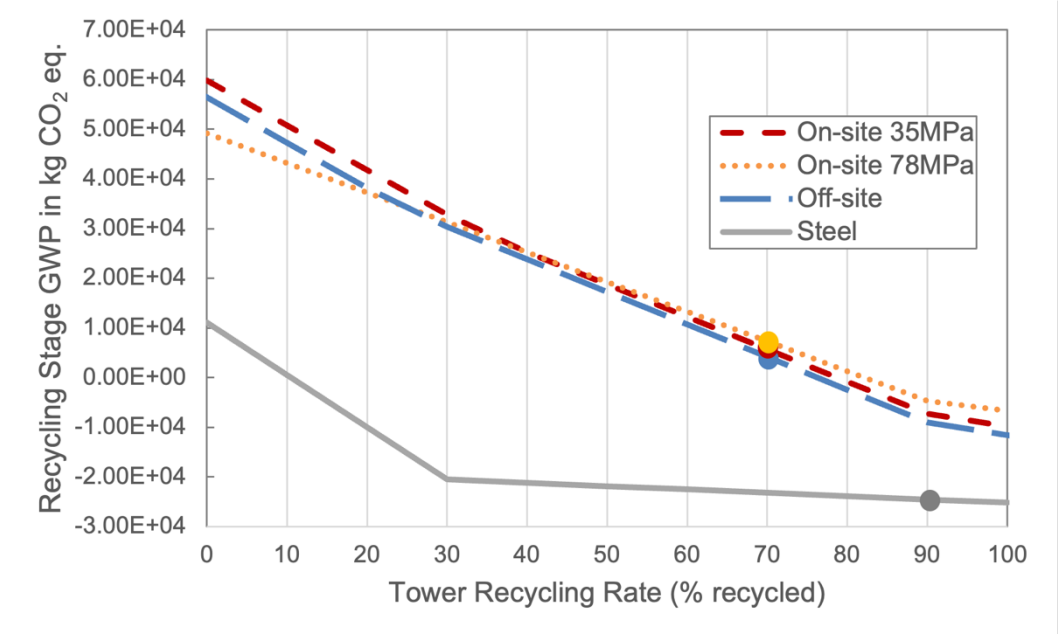

Figure 15 - End of Life stage parameter variation.

Analyzing Figure 15 there are notable shifts in slope whenever the recycling limit of a specific material is reached, which is a representation of the fact that past the recycling limits of that material any excess recycled material is not credited within the original tower. Instead, the benefit of recycling past those percentages is to offset the emissions caused by adding the material into the inert landfill. This analysis does not give additional credit for the recycled materials not originally used within the towers, so while there may be additional emissions advantages to recycling, they are not related to the cradle to grave life cycle of the towers themselves. Based on this parametric study it appears that the recovery of steel from printed towers is the greatest potential emissions offset, as the recycled steel provides notably more emissions offset than the gravel.

5. Summary and Conclusions

In this study, a life cycle assessment was performed on four 140 m tall onshore wind turbine towers: a conventional tubular steel tower assembled using bolted connections, a concrete tower with segments prefabricated Off-site with high-strength (78 MPa) 3D concrete printed shells and precast with normal-strength (35 MPa) concrete and assembled onsite, a concrete tower additively manufactured On-site using normal-strength (35 MPa) concrete, and a concrete tower additively manufactured On-site using high-strength (78 MPa) concrete. The assessment covered five stages of the cradle-to-grave life cycle process of the towers: materials production, transportation, construction, use, and end of life. A comprehensive analysis was performed for each tower to quantify six environmental impact categories.

The life cycle assessment revealed that the concrete tower additively manufactured On-site with normal-strength (35 MPa) concrete had the lowest GWP while the steel tower and the concrete tower prefabricated Off-site and assembled On-site had similar GWP, finally followed by the concrete tower additively manufactured On-site with high-strength (78 MPa) concrete. Compared with the steel tower, the concrete tower additively manufactured On-site with 35 MPa concrete will have 24% lower CO_2 equivalent emissions and 26% higher energy consumption; however, the concrete tower additively manufactured On-site with 78 MPa concrete will have 15% higher CO_2 equivalent emissions and 62% higher energy consumption than the steel tower. From these results, further analyses were performed in order to ascertain the primary contributing factors for each tower's global warming potential. For all four towers the material stage dominated, and was found to contribute over 92% of the total GWP and 67-93% of the life cycle energy consumptions for each tower. This is due to the large volume of materials used for the ultra-tall towers, and relatively low need for repairs and maintenance during the tower's life cycle. Breaking down the GWP of each tower by its material inventory, it was revealed that the cement content in the 3D printed concrete or precast concrete contributed the most towards the GWP of the concrete towers. These findings explain why the On-site tower with 78 MPa concrete has higher life cycle CO_2 equivalent emissions and energy consumption compared to the On-site tower with 35 MPa concrete, because the former contains a significantly higher amount of cement in the concrete by weight. The results also show that compared with a concrete tower with sections prefabricated Off-site and assembled onsite, a 35 MPa concrete tower that is additively manufactured On-site has a 25% reduction in CO_2 equivalent emissions attributed to both the transportation and materials phases.

In addition, a parametric study was performed on each stage of the life cycle process to investigate the effects of certain variables on the global warming potential of the towers within each stage. The variables included the cement content, the distance from the concrete plant to tower construction site, the size and number of tower segments, rated tower life, and tower end-of-life recycling rate. The parametric study quantified the effect of the material's cement ratio on the environmental impact of the towers within the material production stage, examined the impact of transportation distance and tower segment size within the manufacturing stage, and also highlighted aspects of the end-of-life stage based on recycling rates of steel and concrete parts.

The results highlight the need for future development of environmentally friendly 3D printing concrete materials for ultra-tall tower applications. Low-energy and low-CO_2 concrete that incorporates waste or recycled products and can be additively manufactured will significantly reduce the environmental impacts of ultra-tall turbine towers. If the 3D printing concrete can possess high strength, it will also lead to more efficient structural designs that use less concrete, further reducing the environmental impacts. The results from this study reveal an opportunity for further research and development of concrete additive manufacturing technology for wind energy applications including towers, foundations and energy storage.

Future investigations into the life cycle assessment of tall wind turbine towers should also consider more modern tower designs such as hybrid towers, welded steel towers, and more efficiently designed concrete towers made using less concrete or cement, to reflect a more accurate analysis of current industry trends and future practices. It is also proposed that future concrete tower designs incorporating high strength 3D printed concrete should optimize structural designs that minimize the total volume of printed concrete, be it by printing with larger areas of empty space or utilizing shell designs that minimize total surface area. Furthermore, the results of this

study suggest that future development of novel 3D printed concrete materials with lower cement content by volume should be considered for future life cycle assessment of 3D printing concrete structures.

References

[1] Fagan, M., & Huang, C. (2020, October 16). *Many globally are as concerned about climate change as about the spread of infectious diseases*. Pew Research Center. https://www.pewresearch.org/fact-tank/2020/10/16/many-globally-are-as-concerned-about-climate-change-as-about-the-spread-of-infectious-diseases/

[2] Funk, C., & Kennedy, B. (2020, April 21). *How Americans see climate change and the environment in 7 charts*. Pew Research Center. https://www.pewresearch.org/fact-tank/2020/04/21/how-americans-see-climate-change-and-the-environment-in-7-charts/

[3] Gilfillan, D. and Marland, G.: CDIAC-FF: global and national CO_2 emissions from fossil fuel combustion and cement manufacture: 1751–2017, Earth Syst. Sci. Data, 13, 1667–1680, https://doi.org/10.5194/essd-13-1667-2021, 2021.

[4] IPCC, 2014: *Climate Change 2014: Synthesis Report. Contribution of Working Groups I, II and III to the Fifth Assessment Report of the Intergovernmental Panel on Climate Change* [Core Writing Team, R.K. Pachauri and L.A. Meyer (eds.)]. IPCC, Geneva, Switzerland, 151 pp.

[5] "US Wind Power Grew 8 Percent in 2018 amid Record Demand." *AWEA*, American Wind Energy Association, 9 Apr. 2019, www.awea.org/2018-market-report_us-wind-power-grew-8-percent-in-2018.

[6] Wiser, R., Bolinger, M., & Lawrence Berkely National Laboratory. (n.d.). *Land-Based Wind Market Report: 2021 Edition*. U.S. Department of Energy. https://www.energy.gov/sites/default/files/2021-08/Land-Based%20Wind%20Market%20Report%202021%20Edition_Full%20Report_FINAL.pdf

[7] Eric Lantz, Owen Roberts, and Katherine Dykes, “Trends, Opportunities, and Challenges for Tall Wind Turbine and Tower Technologies” NREL, Golden, CO, June 28, 2017. https://www.nrel.gov/docs/fy17osti/68732.pdf

[8] *Wind turbines: The bigger, the better*. (2021, August 30). Energy.gov. https://www.energy.gov/eere/articles/wind-turbines-bigger-better

[9] Cotrell, Jason, Jenne, Scott, and Butterfield, Sandy. “3D Concrete Printing Concept Could Solve Tall-Wind Dilemma”. United States. 2016. https://www.osti.gov/servlets/purl/1337883.

[10] WINDExchange: California potential wind capacity chart. (2015, February). WINDExchange. Retrieved May 12, 2022, from https://windexchange.energy.gov/maps-data/14

[11] Zayas, J., Derby, M., Gilman, P., Ananthan, S., Lantz, E., Cotrell, J., Beck, F., & Tusing, R. (2015). *Enabling Wind Power Nationwide*. U.S. Department of Energy. https://www.energy.gov/sites/default/files/2015/05/f22/Enabling%20Wind%20Power%20Nationwide_18MAY2015_FINAL.pdf

[12] Lantz, E., Roberts, O., Nunemaker, J., DeMeo, E., Dykes, K., & Scott, G. (2019). *Increasing wind turbine tower heights: Opportunities and challenges* (NREL/TP-5000-73629). https://www.nrel.gov/docs/fy19osti/73629.pdf

[13] Bortolotti, P., Johnson, N., Abbas, N. J., Anderson, E., Camarena, E., and Paquette, J.: Land-based wind turbines with flexible rail-transportable blades – Part 1: Conceptual design and aeroservoelastic performance, Wind Energ. Sci., 6, 1277–1290, https://doi.org/10.5194/wes-6-1277-2021, 2021.

[14] Dykes, K., Damiani, R., Roberts, O., and Lantz, E.: Analysis of Ideal Towers for Tall Wind Applications, 2018 Wind Energy Symposium, 8–12 January 2018, Kissimmee, Florida, https://doi.org/10.2514/6.2018-0999, 2018.

[15] Free Documentary. (2020, February 28). *The Making of a Wind Turbine | Exceptional Engineering | Free Documentary* [Video]. YouTube. https://www.youtube.com/watch?v=8NXLKRW1IEU

[16] Gervásio, H., Rebelo, C., Moura, A., Veljkovic, M., & Simões da Silva, L. (2014). Comparative life cycle assessment of tubular wind towers and foundations – Part 2: Life cycle analysis. *Engineering Structures*, *74*, 292-299. https://doi.org/10.1016/j.engstruct.2014.02.041

[17] Levine, A., & Cook, J. (2016). *Transportation of Large Wind Components: A Permitting and Regulatory Review* (NREL/TP-6A20-66998). National Renewable Energy Laboratory. https://www.nrel.gov/docs/fy16osti/66998.pdf

[18] Sritharan, S. (2015). Wind turbine towers: Precast concrete Hexcrete may help increase renewable energy capacity with taller hub heights. *PCI Journal*, *60*(6). https://doi.org/10.15554/pcij60.6-01

[19] *Iowa state engineers test taller wind turbine towers made from precast concrete*. (2015, November 10). News Service • Iowa State University. https://www.news.iastate.edu/news/2015/11/10/tallertowers

[20] Sritharan, Sri. *Hexcrete Tower for Harvesting Wind Energy at Taller Hub Heights – Budget Period 2*. United States: N. p., 2017. Web. Doi:10.2172/1361022.

[21] *Technology — Keystone*. (2021). Keystone. https://keystonetowersystems.com/technology

[22] *Onshore — Keystone*. (2021). Keystone. https://keystonetowersystems.com/onshore

[23] Martínez, E., Sanz, F., Pellegrini, S., Jiménez, E., & Blanco, J. (2009). Life cycle assessment of a multi-megawatt wind turbine. *Renewable Energy*, *34*(3), 667-673. https://doi.org/10.1016/j.renene.2008.05.020

[24] Tremeac, B., & Meunier, F. (2009). Life cycle analysis of 4.5 MW and 250 W wind turbines. *Renewable and Sustainable Energy Reviews*, *13*(8), 2104-2110. https://doi.org/10.1016/j.rser.2009.01.001

[25] Stavridou, N., Koltsakis, E., & Baniotopoulos, C. C. (2019). A comparative life-cycle analysis of tall onshore steel wind-turbine towers. Clean Energy, 4(1), 48-57. https://doi.org/10.1093/ce/zkz028

[26] Rebelo, C., Moura, A., Gervásio, H., Veljkovic, M., & Simões da Silva, L. (2014). Comparative life cycle assessment of tubular wind towers and foundations – Part 1: Structural design. *Engineering Structures*, *74*, 283-291. https://doi.org/10.1016/j.engstruct.2014.02.040

[27] ISO 14040. Environmental management – life cycle assessment – principles and framework. In: International organization for standardization. Geneva, Switzerland; 2006.

[28] ISO 14044. Environmental management – life cycle assessment – requirements and guidelines. In: International organization for standardization. Geneva, Switzerland; 2006.

[29] *BAR: Big adaptive rotor project*. (n.d.). National Renewable Energy Laboratory (NREL) NREL. Retrieved January 5, 2022, from https://www.nrel.gov/wind/big-adaptive-rotor.html

[30] Ptrbortolotti. (2021, April 23). *BAR_Designs/BAR_USC.yaml at NREL/BAR_Designs*. GitHub. Retrieved January 5, 2022,

from https://github.com/NREL/BAR_Designs/blob/6f05ccdf6703be7d2583a9ab9a39edaf05529cac/BAR_USC/BAR_USC.yaml#L442

[31] NREL. (2019). *WISDEM ® documentation — WISDEM 2.0 documentation*. WISDEM ® Documentation — WISDEM 2.0 documentation. Retrieved January 5, 2022, from https://wisdem.readthedocs.io/en/master/index.html

[32] CalPortland Company. (2020). EPD for concrete produced at 8 CalPortland California Facilities (NRMCAEPD: 20035). https://www.nrmca.org/wp-content/uploads/2020/08/CalportlandCaliforniaNRMCAEPD20035.pdf

[33] Liebherr. (2020). *LR11000 Mobile and Crawler Cranes*. pp. 5. Retrieved January, 13, 2022, from https://www.liebherr.com/external/products/products-assets/245502/liebherr-235-lr-11000-td-235-03-defisr11-2020.pdf

[34] United States. Environmental Protection Agency. Office of Transportation and Air Quality. Assessment and Standards Division. (2010). *Median life, annual activity, and load factor values for Nonroad engine emissions modeling*.

[35] World Steel Association. (2017). *LIFE CYCLE INVENTORY METHODOLOGY REPORT*. https://worldsteel.org/wp-content/uploads/Life-cycle-inventory-methodology-report.pdf

[36] Bowyer, J., Bratkovich, S., Fernholz, K., Frank, M., Groot, H., Howe, J., & Pepke, E. (2015, March 23). *UNDERSTANDING STEEL RECOVERY AND RECYCLING RATES AND LIMITATIONS TO RECYCLING*. Dovetail Partners. https://www.dovetailinc.org/report_pdfs/2015/dovetailsteelrecycling0315.pdf

[37] Wernet, G., Bauer, C., Steubing, B., Reinhard, J., Moreno-Ruiz, E., and Weidema, B., 2016. The ecoinvent database version 3 (part I): overview and methodology. The

International Journal of Life Cycle Assessment, [online] 21(9), pp.1218–1230. Available at: <http://link.springer.com/10.1007/s11367-016-1087-8> [Accessed November 2021]. Note: Data entry "Concrete, 35MPa {RoW}| concrete production 35MPa, RNA" accessed via SimaPro ver. 9.0.0.

[38] U.S. Department of Energy. (2021, August 30). Land-Based Wind Market Report: 2021 Edition. https://doi.org/10.2172/1818841

[39] Hasanbeigi, A., Arens, M., Cardenas, J. C., Price, L., & Triolo, R. (2016). Comparison of carbon dioxide emissions intensity of steel production in China, Germany, Mexico, and the United States. Resources, Conservation and Recycling, 113, 127-139. https://doi.org/10.1016/j.resconrec.2016.06.008

[40] Kuzmenko, K., Feraille, A., Baverel, O., & Roussel, N. (2020). Environmental impacts of 6-Axes robotic arm for 3D concrete printing. *RILEM Bookseries*, 1023-1030. https://doi.org/10.1007/978-3-030-49916-7_99

[41] Thomson, R. C., Chick, J. P., & Harrison, G. P. (2018). An LCA of the Pelamis wave energy converter. *The International Journal of Life Cycle Assessment*, *24*(1), 51-63. https://doi.org/10.1007/s11367-018-1504-2
Relevant supplementary material accessed: https://static-content.springer.com/esm/art%3A10.1007%2Fs11367-018-1504-2/MediaObjects/11367_2018_1504_MOESM1_ESM.pdf

[42] Hempel. (2022, March). *Hempadur 4774D*. hempel.com. Retrieved December 8, 2021, from https://www.hempel.com/api/Hempel/DataSheet/PDS/Download/4774D/en-GB

[43] Hempel. (2022, March). *Hempathane HS 5561B*. hempel.com. Retrieved December 8, 2021, from https://www.hempel.com/api/Hempel/DataSheet/PDS/Download/5561B/en-GB

[44] Hempel. (2021, November 13). *Hempadur 4774M Base*. hempel.com. Retrieved December 8, 2021, from https://www.hempel.com/api/Hempel/DataSheet/SDS/Download/4774M17130/Europe/en-US

[45] Hempel. (2021, November 16). *Hempel's Curing Agent 9874D*. hempel.com. Retrieved December 8, 2021, from https://www.hempel.com/api/Hempel/DataSheet/SDS/Download/9874D00000/Europe/en-US

[46] Hempel. (2022, February 2). *Hempel's Thinner 08450*. hempel.com. Retrieved December 8, 2021, from https://www.hempel.com/api/Hempel/DataSheet/SDS/Download/0845000000/Europe/en-US

[47] Hempel. (2021, November 14). *Hempathane HS 5561P Base*. hempel.com. Retrieved December 8, 2021, from https://www.hempel.com/api/Hempel/DataSheet/SDS/Download/5561P10170/Europe/en-US

[48] Hempel. (2021, November 16). *Hempel's Curing Agent 97050*. hempel.com. Retrieved December 8, 2021, from https://www.hempel.com/api/Hempel/DataSheet/SDS/Download/9705000000/Europe/en-US

[49] Hempel. (2021, November 12). *Hempel's Thinner 08080*. hempel.com. Retrieved December 8, 2021, from https://www.hempel.com/api/Hempel/DataSheet/SDS/Download/0808000000/Europe/en-US

Appendix A.

Table A.1 - Details of the towers studied in the LCA with their corresponding Simapro inventory selections.

Process or material	Quantity	Unit	Selected Inventory Process/emission
Segmented Steel Tower	**1**	**p**	
Tower body	738	ton	Steel welded pipe/GLO
Flanges	152	ton	Steel sections/GLO
Bolts	23.2	ton	Steel wire rod/GLO
Primer	5.19E+03	m2	Painting, epoxy primer
Topcoat	2.61E+03	m2	Painting, topcoat
Worker transportation	2.00E+04	pmi	Transport, passenger car, gasoline powered/personkm/RNA
Material transportation	1.49E+06	tkm	Transport, combination truck, long-haul, diesel powered, West/tkm/RNA
Crane operation	5.00	hr	Machine operation, diesel, >= 74.57 kW, steady-state {GLO}| market for | APOS, U
35 MPa On-Site Concrete Tower	**1**	**p**	
3D printed cement	5.34E+06	kg	35 MPa 3DCP Concrete
Grout*	576932.4	kg	Cement mortar {RoW}| market for cement mortar| APOS, U
Rebar	250	tn.sh	Steel rebar/GLO
Pre-stressing tendons	304000	lb	Steel wire rod/GLO
Connecting Grout	1.61E+04	kg	Cement mortar {RoW}| market for cement mortar| APOS, U
Worker transportation	2.73E+04	pmi	Transport, passenger car, gasoline powered/personkm/RNA
3D Printer operation	7.22E+02	hr	3DCP Printer Run Time
Printer transport	5.55E+02	tkm	Transport, light commercial truck, diesel powered, West/tkm/RNA
Crane operation	46	hr	Machine operation, diesel, >= 74.57 kW, steady-state {GLO}| market for | APOS, U
Material transportation	9.25E+04	tkm	Transport, combination truck, short-haul, diesel powered, West/tkm/RNA
78 MPa On-Site Concrete Tower	**1**	**p**	

3D printed cement	4.05E+06	kg	78 MPa 3DCP Concrete
Grout*	5.84E+05	kg	Cement mortar {RoW}| market for cement mortar| APOS, U
Rebar	2.50E+02	tn.sh	Steel rebar/GLO
Pre-stressing tendons	3.04E+05	lb	Steel wire rod/GLO
Connecting Grout	1.61E+04	kg	Cement mortar {RoW}| market for cement mortar| APOS, U
Worker Transportation	2.73E+04	pmi	Transport, passenger car, gasoline powered/personkm/RNA
3D Printer operation	7.22E+02	hr	3DCP Printer Run Time
Printer transport	5.55E+02	tkm	Transport, light commercial truck, diesel powered, West/tkm/RNA
Crane operation	4.60E+01	hr	Machine operation, diesel, >= 74.57 kW, steady-state {GLO}| market for | APOS, U
Material transportation	8.42E+04	tkm	Transport, combination truck, short-haul, diesel powered, West/tkm/RNA
Off-Site Concrete Tower	**1**	**p**	
3D printed cement	2.15E+06	kg	78 MPa 3DCP Concrete
Grout*	255667.15	kg	Cement mortar {RoW}| market for cement mortar| APOS, U
Rebar	250	tn.sh	Steel rebar/GLO
Pre-stressing tendons	304000	lb	Steel wire rod/GLO
Ready-mix concrete	2059	cu.yd	35MPa Concrete CalPortland Mix 45EF6Z**
Connecting Grout	1.19E+04	kg	Cement mortar {RoW}| market for cement mortar| APOS, U
Worker transportation	2.06E+04	pmi	Transport, passenger car, gasoline powered/personkm/RNA
3D Printer operation	2.85E+02	hr	3DCP Printer Run Time
Printer transport	2.66E+02	tkm	Transport, light commercial truck, diesel powered, West/tkm/RNA
Crane operation	12	hr	Machine operation, diesel, >= 74.57 kW, steady-state {GLO}| market for | APOS, U
Material transportation	6.68E+05	tkm	Transport, combination truck, short-haul, diesel powered, West/tkm/RNA

*Assumed 2200kg/m^3 density

**From CalPortland Company, (2020). [32]

Table A.2 – Emissions category used for printer run time calculations.

Process or material	Quantity	Unit	Selected Inventory Process/emission
3DCP Printer Run Time	**1**	**hr**	
Machine running*	20	personkm	Transport, passenger car, diesel powered/persomkm/RNA

*Modeled after XtreeeE printing system for a single hour use of one 6-axis 3D printer. [40]

Table A.3 - Details of the printed concrete materials used in the printed tower designs with their corresponding Simapro inventory selections.

Process or material	Quantity	Unit	Selected Inventory Process/emission
78 MPa 3DCP Concrete*	**17898.5**	**g**	
Cement	8500	g	Cement, Portland {US}| market for
Sand	5000	g	Silica sand {GLO}| market for
Water	2650	g	Tap water {RoW}|tap water production, conventional treatment
Super Plasticiser	145	g	Plasticiser, for concrete, based on sulfonated melamine formaldehyde {GLO}| market for
VMA	5	g	1-butanol {RoW}| hydroformylation of propylene
Retarder	8.5	g	Plasticiser, for concrete, based on sulfonated melamine formaldehyde {GLO}| market for
Transport	-	tkm	Transport by weight taken from Concrete, 50MPa {GLO}| market for
35 MPa 3DCP Concrete*	**2321.1**	**kg**	
Cement	338	kg	Cement, Portland {US}| market for
Sand	780	kg	Silica sand {GLO}| market for
Gravel	880	kg	Gravel, round {RoW}| market for
Water	200	kg	Tap water {RoW}|tap water production, conventional treatment
Superplasticiser	5	kg	Plasticiser, for concrete, based on sulfonated melamine formaldehyde {GLO}| market for
Stiffener	1.5	kg	1-butanol {RoW}| hydroformylation of propylene

Accelerator		4.6	kg	Calcium nitrate {GLO}| market for
Transport	-		tkm	Transport by weight taken from Concrete, 50MPa {GLO}| market for

*Masses of silica fume not included due to the material's status as a waste byproduct

Table A.4 - Details of the paint materials used in steel tower coatings with their corresponding Simapro inventory selections. Technique adapted from the supplemental materials of [41].

Process or material	Quantity	Unit	Uncertainty	Selected Inventory Process/emission
Painting, epoxy primer	**m2**			
Epoxy paint primer	0.294	kg		Detailed below.
Compressed air supply for painting [41]	3.268	m3		Compressed air, 700 kPa gauge {GLO}| market for
Painting, topcoat	**m2**			
Topcoat	0.14	kg		Detailed below.
Compressed air supply for painting [41]	1.667	m3		Compressed air, 700 kPa gauge {GLO}| market for
Epoxy paint primer [42]	**kg**			
HEMPADUR 4774D Base: 4774M-17130	0.852	kg		Detailed below.
HEMPADUR 4774D Curing Agent: 9874D	0.125	kg		Detailed below.
Thinner 08450/D **5%-10%** (to dilute the epoxy for appl.)	0.00429	kg		Detailed below.
Topcoat [43]	**kg**			
HEMPATHANE HS 5561B Base: 5561P	0.875	kg		Detailed below.
HEMPATHANE HS 5561B Curing Agent: 97050	0.101	kg		Detailed below.
Thinner 08080 **10%-20%** (to dilute urethane for appl.)	0.0932	kg		Detailed below.
Base 4774M [44]	**kg**			
Titanium dioxide	0.175	kg	0.1 - 0.25	Titanium dioxide {RoW} | APOS,U

bispenol A-(epichlorhydrin) epoxy resin MW =<700	0.13	kg	0.1 - 0.16	Epoxy resin, liquid {RoW} | market for
xylene	0.075	kg	0.05 - 0.1	Xylene {RoW}| market for
oxirane, mono[(C12-14-alkyloxy)methyl] derivs.	0.075	kg	0.05 - 0.1	Alkyl sulphate (C12-14) {GLO}| market for
middle molecular epoxy resin MMW 700-1200	0.0665	kg	0.05 - 0.083	Epoxy resin, liquid {RoW} | market for
butan-1-ol	0.02	kg	0.01 - 0.03	1-butanol {GLO}|market for
ethylbenzene	0.02	kg	0.01 - 0.03	Ethyl benzene {RoW}| market for
1,3-bis(12-hydroxyocta-decanamide-N-methyle) benzene	0.01	kg	0.01	Dimethenamide {GLO}| market for
C12-14 alcohols	0.003	kg	0.003	Fatty alcohol {GLO}|market for
toluene	0.003	kg	0.003	Toluene, liquid {RoW}| market for
Remainder	0.4225	kg	0.231 - 0.614	Epoxy resin, liquid {RoW} | market for
Curing Agent 9874D [45]	**kg**			
xylene	0.175	kg	0.1-0.25	Xylene {RoW}| market for
butan-1-ol	0.15	kg	0.1-0.2	1-butanol {GLO}|market for
2,4,6-tris(dimethylaminomethyl)phenol	0.075	kg	0.05 - 0.1	O-aminophenol {GLO}| market for
ethylbenzene	0.04	kg	0.03 - 0.05	Ethyl benzene {RoW}| market for
3,6-diazaoctanethylenediamin	0.02	kg	0.01 - 0.03	Diethylene glycol {GLO}| market for
bis[(dimethylamino)methyl]phenol	0.02	kg	0.01 - 0.03	O-aminophenol {GLO}| market for
salicylic acid	0.01	kg	0.01	Salicylic acid {GLO}| market for
toluene	0.003	kg	0.003	Toluene, liquid {RoW}| market for
Remainder	0.507	kg	0.327 - 0.687	Epoxy resin, liquid {RoW} | market for
Thinner 08450 [46]	**kg**			
xylene	0.625	kg	0.5 - 0.75	Xylene {RoW}| market for
butan-1-ol	0.175	kg	0.1 - 0.25	1-butanol {GLO}|market for

ethylbenzene	0.175	kg	0.1 - 0.25	Ethyl benzene {RoW}| market for
solvent naphtha (petroleum), light arom.	0.175	kg	0.1 - 0.25	Naphtha {RoW}| market for
toluene	0.01	kg	0.01	Toluene, liquid {RoW}| market for
Remainder				
Base 5561P [47]	**kg**			
Titanium dioxide	0.175	kg	0.1 - 0.25	Titanium dioxide {RoW} | APOS,U
solvent naphtha (petroleum), light arom.	0.075	kg	0.05 - 0.1	Naphtha {RoW}| market for
solvent naphtha (petroleum), light arom.	0.0695	kg	0.05 - 0.089	Naphtha {RoW}| market for
n-butyl acetate	0.075	kg	0.05 - 0.1	Butyl acetate {RoW}| market for
xylene	0.02	kg	0.01 - 0.03	Xylene {RoW}| market for
ethylbenzene	0.02	kg	0.01 - 0.03	Ethyl benzene {RoW}| market for
reaction mass of bis (1,2,2,6,6-pentamethyl-4-piperidyl) sebacate and methyl 1,2,2,6,6-pentamethyl-4-priperidyl sebacate	0.0046	kg	0.0046	1-pentanol {GLO}| market for
trimethylolpropane	0.003	kg	0.003	Trimethylamine {RoW}| market for
Remainder	0.5579	kg	0.3934 - 0.7224	Epoxy resin, liquid {RoW} | market for
Curing Agent 97050 [48]	**kg**			
hexamethylene-1,6-diisocyanate homopolymer	0.825	kg	0.75 - 0.90	Methylene diphenyl diisocyanate {RoW}| market for
n-butyl acetate	0.075	kg	0.05 - 0.1	Butyl acetate {RoW}| market for
solvent naphtha (petroleum), light arom.	0.04	kg	0.03 - 0.05	Naphtha {RoW}| market for
hexamethylene-di-isocyanate	0.003	kg	0.003	Methylene diphenyl diisocyanate {RoW}| market for
Remainder	0.057	kg	0 - 0.167	Epoxy resin, liquid {RoW} | market for
Thinner 08080 [49]	**kg**			
xylene	0.825	kg	0.75 - 0.9	Xylene {RoW}| market for

ethylbenzene	0.175	kg	0.1 - 0.25	Ethyl benzene {RoW}| market for
toluene	0.02	kg	0.01 - 0.03	Toluene, liquid {RoW}| market for